

## Article

# Two Red Sea Sponge Extracts (*Negombata magnifica* and *Callyspongia siphonella*) Induced Anticancer and Antimicrobial Activity

Hussein A. El-Naggar <sup>1,\*</sup>, Mansour A. E. Bashar <sup>1</sup>, Islam Rady <sup>1,\*</sup>, Mohammad S. El-Wetidy <sup>2</sup>,  
Waleed B. Suleiman <sup>3,\*</sup>, Fatimah O. Al-Otibi <sup>4</sup>, Sara A. Al-Rashed <sup>4</sup>, Lamiaa M. Abd El-Maoula <sup>5</sup>,  
El-Sayed S. Salem <sup>6</sup>, Enas M. H. Attia <sup>7</sup> and Sayed Bakry <sup>1</sup>

<sup>1</sup> Zoology Department, Faculty of Science, Al-Azhar University, Nasr City, Cairo 11884, Egypt; dr\_mb2020682@azhar.edu.eg (M.A.E.B.); sbakry@azhar.edu.eg (S.B.)

<sup>2</sup> College of Medicine Research Center, King Saud University, Riyadh 11451, Saudi Arabia; melwatidy@ksu.edu.sa

<sup>3</sup> Botany and Microbiology Department, Faculty of Science, Al-Azhar University, Nasr City, Cairo 11884, Egypt

<sup>4</sup> Department of Botany and Microbiology, College of Science, King Saud University, Riyadh 11451, Saudi Arabia; falotibi@ksu.edu.sa (F.O.A.-O.); salrashed@ksu.edu.sa (S.A.A.-R.)

<sup>5</sup> Nutrition and Food Science Department, Faculty of Home Economics, Al-Azhar University, Tanta 31732, Egypt; dr\_lamiaamostafa@azhar.edu.eg

<sup>6</sup> Environmental Egyptian Affairs Agency, Red Sea Protectorates Sector, Hurghada 84511, Egypt; elsayed\_salm@yahoo.com

<sup>7</sup> Physics Department, Faculty of Science, Al-Azhar University, Nasr City, Cairo 11823, Egypt; Drenas\_attia\_biophysics@azhar.edu.eg

\* Correspondence: hu\_gar2000@azhar.edu.eg (H.A.E.-N.); islamrady@azhar.edu.eg (I.R.); dr\_wbs@azhar.edu.eg (W.B.S.)



**Citation:** El-Naggar, H.A.; Bashar, M.A.E.; Rady, I.; El-Wetidy, M.S.; Suleiman, W.B.; Al-Otibi, F.O.; Al-Rashed, S.A.; Abd El-Maoula, L.M.; Salem, E.-S.S.; Attia, E.M.H.; et al. Two Red Sea Sponge Extracts (*Negombata magnifica* and *Callyspongia siphonella*) Induced Anticancer and Antimicrobial Activity. *Appl. Sci.* **2022**, *12*, 1400. <https://doi.org/10.3390/app12031400>

**Academic Editors:** Alessandra Durazzo and Maria Stefania Sinicropi

Received: 16 September 2021

Accepted: 20 January 2022

Published: 28 January 2022

**Publisher's Note:** MDPI stays neutral with regard to jurisdictional claims in published maps and institutional affiliations.



**Copyright:** © 2022 by the authors. Licensee MDPI, Basel, Switzerland. This article is an open access article distributed under the terms and conditions of the Creative Commons Attribution (CC BY) license (<https://creativecommons.org/licenses/by/4.0/>).

**Abstract:** Bioactive compounds extracted from marine organisms showed several biological activities. The present study is an extension of our earlier studies where we assessed the antiproliferative and pro-apoptotic activities of ethanol, methylene chloride, ethyl acetate, acetone, and chloroform crude extracts of sponges: *Negombata magnifica* (NmE) and *Callyspongia siphonella* (CsE) against cancer cells. Herein, we are extending our previous findings on both sponge species depending on an alternative methanol extraction method with more advanced molecular biochemical insights as additional proof for anticancer and antimicrobial activity of *N. magnifica* and *C. siphonella*. Therefore, sponge specimens were collected during winter 2020 from the Dahab region at the Gulf of Aqaba. Each sponge was macerated with methanol to obtain the crude extracts; NmE and CsE. GC-MS analysis presented a total of 117 chemical compounds; 37 bioactive, 11 represented previously as constituents for a natural organism, and 69 had no biological activities. NmE dose-dependently inhibited the growth of HepG2, MCF-7, and Caco-2 carcinoma cell lines compared to CsE, which unfortunately has no antiproliferative activity against the same cancer cells. NmE was found to induce G0/G1 cell cycle arrest in HepG2 cells with its inhibition for CDK6, Cyclins D1, and E1 in HepG2, MCF-7, and Caco-2 cells. NmE also activated ROS production in HepG2 cells and induced apoptosis in HepG2, MCF-7, and Caco-2 cells via an increase in pro-apoptotic protein Bax, caspase-3, and cleavage PARP, and a decrease in anti-apoptotic protein BCL2. Unlike its anticancer potential, CsE exhibited clear superior results as an antimicrobial agent with a wider range against six microbial strains, whereas NmE showed a positive antibacterial activity against only two strains.

**Keywords:** sponges; *Negombata magnifica*; *Callyspongia siphonella*; Red Sea; anticancer; antimicrobial

## 1. Introduction

Marine species have had a lot of success in the last several years as a source of novel bioactive chemicals for medication development [1]. As a result, since the middle of the

twentieth century, several scientists have attempted to identify novel active chemicals from marine species [2]. The scientists have increasingly been focusing their marine studies on the deepwater [3], so it is reasonable to expect increases in the active chemicals extracted from deep-sea creatures [4]. The Red Sea contains a hugely diverse range of micro- and macroorganisms [5–7], most of them have been unexplored until now. Up to 58 new endemic species have been discovered in the Red Sea in the previous two decades [8].

On the other hand, because of the worrisome increase in the incidence of cancer diseases [9,10] and other emerging diseases, such as COVID-19 [11,12], there is an urgent need to identify new bioactive chemicals. As a result, the output of natural medical products from the oceans is greatly assisting the present study trend of natural drug discovery theory, as the seas have the most biological and chemical diversity of all our planet's ecosystems [13,14].

Bioactive chemicals obtained from the sea have promising options for treating human ailments, including cancer. For example, no fewer than 3000 marine active components have been tested for their anticancer activity in the recent past [15,16]. Furthermore, antioxidant, anti-inflammatory, antimicrobial, anticoagulant, immune-stimulatory, anti-hypertension, and wound healing action have been demonstrated in marine bioactive chemicals isolated from marine creatures [17]. Because of their soft bodies and sedentary habits, marine sponges (Phylum: Porifera) are the most abundant and diverse marine organisms [18].

The sponges of the Red Sea contain a variety of bioactive chemicals that have a variety of therapeutic benefits [19–23]. Anticancer action was found in cyclic peroxide norterpenoids derived from the Red Sea sponge *Diacarnus erythraeanus* [24]. Accordingly, bioactive components produced from the Red Sea sponge *Theonella swinhoei*, such as Swinholide and hurghadolide [25] and Theonellamide [26], exhibit antifungal action, and also inhibit the HCT-116 cancer cell line. Toxiusol, shaagrocol, and toxicols, hexaprenoid hydroquinones derived from the Red Sea sponge *Toxiclona toxius*, showed antiviral activity against HIV-1 [27]. Subereaphenol was extracted from the Red Sea sponge *Suberea mollis* and was shown to inhibit cell proliferation in the HeLa cancer cell line [28]. 19-hydroxypsammaphysins and psammaphysins that were isolated from *Aplysinella* sp. displayed cytotoxic activities against HeLa cell and MBA-MB-231 [29].

From sponge *Hyrtios erectus*, two indole alkaloids exhibited HeLa cancer cells [30], while sesterterpenes derived from the same sponge have significant cytotoxicity to HT-29, P-388, and A-549 cancer cells [31], and antiproliferative activities against HepG2, HCT-116, and MCF-7 cancer cells [32]. As marine metabolites purified from the Red Sea sponge *Raspailia* sp. induced cytotoxicity against MEL-28, HT-29, A-549, and P-388 cancer cells [33]. Actinomycetes isolated from *Sphaciospongia vagabunda* have antioxidant activities and protective anticancer properties from the genomic damage produced by H<sub>2</sub>O<sub>2</sub> in HL-60 cancer cell line [34]. Scrobiculosides derived from *Pachastrella scrobiculosa* exhibited anticancer activities against P388 and HL-60 cancer cells [35]. Discorhabdin alkaloids purified from sponge *Latrunculia biformis* showed in vitro anticancer activities [36]. Many active chemicals from deep-sea sponges *Iophon methanophila* and *Hymedesmia methanophila* showed antimicrobial activities [37]. In the same context, *Callyspongia siphonella* has many bioactive components such as Neviotane triterpene, and metabolites that induce anticancer activities against A549, PC-3, and MCF-7 cancer cells [38], two brominated oxindole alkaloids induced anticancer activities, and antimicrobial against Gram-positive bacteria [39]. Dehydroisophonochalynol, callyspongenol, and the C22-polyacetylenic alcohols callyspongenol were isolated from sponge *Callyspongia* sp. and showed cytotoxicity against HeLa and P388 cancer cells [40]. Polyacetylenic amide (callyspongamide) purified from *Callyspongia fistularis* exhibited cytotoxic activities against HeLa cancer cells [41]. Gelliusterol isolated from *Callyspongia affImplexa* inhibited chlamydial inclusions [42].

Rady and Bashar, 2020 [1], examined eight extracts of two species of deep-Red Sea sponge: finger-sponge (*Negombata magnifica*) and tube-sponge (*Callyspongia siphonella*) (extracted by four different solvents; CH<sub>2</sub>Cl<sub>2</sub>, C<sub>4</sub>H<sub>8</sub>O<sub>2</sub>, C<sub>3</sub>H<sub>6</sub>O, and CHCl<sub>3</sub>, separately), against HepG2, MCF-7, and Caco-2 cancer cells. Depending on a dose-dependent manner,

they found all extracts inhibited the growth of HepG2, MCF-7, and Caco-2 cancer cells and induced apoptosis in the same cancer cell lines via Bax and caspase-3 increase, and BCL2 decrease. Herein, the present work is an extension of this work, but here we prepare methanolic extracts for same sponge species (*NmE* and *CsE*) and state their bioactive compounds and introduce their anticancer and antimicrobial activities.

## 2. Materials and Methods

### 2.1. Sampling and Identification of Sponge Specimens

The sponge specimens were collected from the Dahab coast, Gulf of Aqaba at 30 m depth by SCUBA diving during winter (February) 2020. The specimens were carefully identified based on Porifera morphological characters according to Systema Porifera [43] associated with the most recent update undertaken in the World Porifera Database [44].

### 2.2. Preparation of *NmE* and *CsE*

This procedure was carried out according to El-naggar and Hasaballah, 2018 [20] with some modifications. Firstly, 100 gm of sponge were macerated with 200 mL of 70% aqueous methanol. The mixture was continuously stirred by a rotary shaker (200 rpm) for one week in dark. Then, the mixtures were filtered through Whatman 542 filter paper, and the solvent was evaporated using a rotary evaporator at 40 °C (LARK, Model: VC-100A) and preserved at −20 °C for further analysis.

### 2.3. GC–MS Analysis of *NmE* and *CsE*

One microliter of each extract was examined for its contents of bioactive compounds using a Gas Chromatography–Mass Spectrometer (Hewlett Packard HP-5890 series II) equipped with a split/splitless injector and a capillary column (30 m, 0.25 mm, 0.25 mL) fused with phenyl polysilphenylene siloxane. The temperatures of injector and detector were set at 280 and 300 °C, respectively, and the oven temperature was kept at 80 °C for 1 min, and rose to 300 °C at 20 °C/min. The helium was used as carrier gas at a constant flow of 1.0 mL/min. A volume of 2 microliter was injected in the splitless mode and the purge time was 1 min. The MS (Hewlett-Packard 5889B MS Engine) with selected ion monitoring (SIM) was used. The mass spectrometer was operated at 70 eV, scanning fragments from 50 to 1000 *m/z*. Peak identification of crude extract was performed based on comparing the obtained mass spectra with those available in the NIST library [45].

### 2.4. Anticancer Assay

#### 2.4.1. Cell Culture

HepG2, MCF-7, and Caco-2 cancer cell lines were obtained from American Type Culture Collection (Manassas, VA, USA) and (VACsERA Co., Cairo, Egypt). Those cancer cells were cultured in DMEM (Corning Thomas Scientific, Swedesboro, NJ, USA). DMSO was purchased from (Sigma-Aldrich, Saint Louis, MO, USA), while FBS was purchased from Hyclone (Pittsburgh, PA, USA) and PSA was obtained from Mediatech Inc. (Herndon, VA, USA). Unless otherwise indicated, cancer cells were cultured in DMEM supplemented with 5% heat-inactivated FBS and 1% PSA at 37 °C in a 5% CO<sub>2</sub> incubator, and the untreated growth media containing vehicle DMSO (0.01%) were used as negative controls for all assays [46].

#### 2.4.2. Measurement of Cytotoxicity by MTT Assay

The cytotoxicity of *NmE* and *CsE* against HepG2, MCF-7, and Caco-2 was measured by Cell Proliferation Kit I MTT (Sigma-Aldrich, Saint Louis, MO, USA). Accordingly, the cells were cultivated in 96 well culture plates at 5000/well for 24 h. Then, cells were provided with different concentrations of *NmE* (0, 6.25, 12.5, and 25 µg/mL) and *CsE* (0, 156.2, 312.5, 625, 1250, and 2500 µg/mL) individually for 48 h in 37 °C and humidity 5% in CO<sub>2</sub> incubator. Treated and untreated Cells were incubated with 10 µL of the MTT powder (final concentration, 0.5 mg/mL) for 2 h after until violet crystals were formed

at different color hues indicating cell metabolic activity. The insoluble formazan crystals are dissolved using a solubilization solution (Phosphate buffered saline). Colorimetric absorbance was measured at 620 nm (A620) and 570 nm (A570) by Synergy™ 2 Multi-Mode Microplate Reader (BioTek Inc., Winooski, VT, USA). The cell viability was calculated using the following equation [47].

$$\text{Percentage of viability} = \frac{\text{A570} - \text{A620 of Extract}}{\text{A570} - \text{A620 of the Control (0}\mu\text{M)}} \times 100$$

The IC<sub>50</sub> was calculated by the IC<sub>50</sub> calculator as previously described by Luparello et al. [48]. The protocols of treatment and analysis were performed at least three times.

Due to the *NmE* potentiality as an antiproliferative active agent, it was chosen for the current investigations.

#### 2.4.3. Protein Extraction and Western Blotting

The medium was discarded 24 h after HepG2, MCF-7, and Caco-2 cells treatment with *NmE*. Then, cells were washed with cold PBS (10 mmol/L, pH 7.4) followed by incubation on an ice-cold lysis buffer (50 mmol/L Tris-HCl, 150 mmol/L NaCl, 1 mmol/L EGTA, 1 mmol/L EDTA, 20 mmol/L NaF, 100 mmol/L Na<sub>3</sub>VO<sub>4</sub>, 0.5% NP40, 1% Triton X-100, 1 mmol/L PMSF (pH 7.4)) with a freshly added inhibitor cocktail (Inhibitor Cocktail Set III, Calbiochem, La Jolla, CA, USA) over ice for 30 min [49]. The cells were scraped, and the suspension was passed many times through a 21.5-gauge needle up and down in a microfuge tube to split up any cell aggregates [50]. Then, centrifugation for lysate at 14,000 × *g* for 25 min at 4 °C, and the total cell lysate (supernatant) was stored at 80 °C for further analysis [49].

Bax, Bcl2, Caspase-3, CDK6, Cyclin D1, cyclin E1, PARP, HRP anti-mouse, and anti-rabbit secondary antibodies were obtained from Cell Signaling Technology (Beverly, MA, USA), whereas GAPDH, β-actin were purchased from Santa Cruz Biotechnology, Inc. (Santa Cruz Co., Santa Cruz, CA, USA). Mini-protean precast Tris-Glycine gels were from BioRad (Hercules, CA, USA). ECL detection system was from GE Healthcare (Buckinghamshire, UK). A 2% (*w/v*) Aqueous Solution of Gentician Violet was from Ricca Chemical Company (Arlington, TX, USA). Invitrogen Novex precast Tris-Glycine gels were from Corning. Briefly, 25–40 μg of protein were resolved over 8%–12% polyacrylamide gels and transferred to a nitrocellulose membrane. The blot was blocked in blocking buffer (7% nonfat dry milk/1% Tween 20; in 20 mmol/L TBS (pH 7.6)) for 1 h at room temperature, incubated with the appropriate monoclonal or polyclonal primary antibody in blocking buffer for 2 h at room temperature or overnight at 4 °C, followed by incubation with an appropriate secondary antibody HRP conjugate. The blots were exposed to enhanced chemiluminescence (Thermo Scientific Pierce, Rockford, IL, USA) and subjected to autoradiography using a BioRad (Hercules, CA, USA) imaging system. The digitalized scientific software program Quantity One (BioRad) was used for the analysis of the Western blot to assess the densitometric measurements of the bands, and treatment protocol was carried out at least three times, as well as each protein expression, was analyzed three times with analogous results [49,50].

#### 2.4.4. Cell Cycle Assay with PI

The effect of *NmE* on HepG2 cell cycle was handled as described by Kim and Sederstrom, 2015 [51]. Briefly, cells were seeded in 6-well plates (3 × 10<sup>5</sup> cells per well) and allowed to attach and grow for 24 h in the mean culture conditions. The cells were treated with *NmE* (0, 6.25, 12.5, and 25 μg/mL) for 24 h. At the time of detection, cells were harvested, and both attached and floating cells were collected. The cells were fixed by slowly dropping the 70% ice-cold ethanol and stored at 4 °C for at least 30 min. Later, the cells were washed twice with ice-cold PBS at 2000 rpm, then incubated in PBS with RNase A (10 mg/mL) (QIAGEN, Hilden, Germany) and PI (50 μg/mL) at room temperature for 10 min. Cell cycles were analyzed using a BD FACSCalibur™ Cell analyzer equipped with

Cell Quest software at an emission of >575 nm (FL3). The area occupied by all the cell cycle phases (Sub G, G0/G1, S, and G2/M phase), expressed in resulting histograms, were measured and graphed together.

#### 2.4.5. Annexin V-FITC/PI Assay

Induction of apoptosis was measured by Dead Cell Apoptosis Kit with Annexin V FITC and PI, for flow cytometry (Invitrogen, by ThermoFischer Scientific, Eugene, OR, USA) according to the manufacturer's instruction. HepG2 cancer cells were seeded in a 96-well plate ( $3 \times 10^5$  cells per well) and treated with the *NmE* (0, 6.25, 12.5, and 25  $\mu\text{g}/\text{mL}$ ) for 24 h. Both floating and adherent cells were harvested, pooled together, and incubated with Annexin V-FITC and PI for 15 min on ice in dark. The cells were analyzed by BD FACSCalibur™ Cell analyzer (BD Biosciences, San Jose, CA, USA) at an emission of 530 nm (FL1 channel) and >575 nm (FL3). The percentage of living cells (negative in both annexin V-FITC and PI), early apoptotic (positive in annexin V-FITC), late apoptotic and completely dead (positive in both annexin V-FITC and PI), and necrotic cells (only positive for PI) were all calculated and graphed together as had been described before by [52].

#### 2.4.6. ROS Assay

The probably oxidative stress effect induced by *NmE* through the ROS production was tested by the DCFDA/H2DCFDA—Cellular ROS Assay Kit (ABCAM, Cambridge, UK) and flow cytometer according to the manufacturer instructions, as described before by Degl'Innocenti et al., 2019 [53]. HepG2 cancer cells were seeded in 6-well plates ( $3 \times 10^5$  cells per well) and allowed to attach for 24 h as described above. The cells were treated with *NmE* (0, 6.25, 12.5, and 25  $\mu\text{g}/\text{mL}$ ) for 24 h. At the detection time, cells were trypsinized, and all attached and floating cells were collected. The cells were, then, treated by DCFDA, and stored at 37 °C for 30 min. Before analysis, the cells were washed twice with ice-cold PBS, analyzed using a flow cytometer at an emission of 530 nm (FL1 channel) and 150 mV.

### 2.5. Antimicrobial Assay

#### 2.5.1. Microbial Indicator Strains

The bacterial indicators were provided by the regional center for mycology and biotechnology, Al-Azhar University. Ten test microorganisms were selected to cover all categories either filamentous fungi, yeasts, or Gram-positive and Gram-negative bacteria as follows: *Aspergillus flavus*, *Penicillium expansum* IMI28169, *Candida lipolytica*, *Cryptococcus neoformans*, *Micrococcus* sp., *Streptococcus mutants* ATCC25175, Methicillin-resistant *Staphylococcus aureus*, *Salmonella typhimurium* ATCC 14028, *Escherichia coli* ATCC 25955, and *Klebsiella pneumonia* ATCC 13883.

#### 2.5.2. Media and Inocula

Mueller–Hinton agar medium was used for bacterial growth assay. It is composed of g/L; beef dehydrated infusion 300, casein hydrolysate 17.5, starch 1.5, and agar 17; this medium is ready to use when it has been prepared by weighing 38 g and up to 1 L distilled water. Furthermore, fungi and yeasts were cultivated onto malt extract agar MEA medium, which is composed of (g/L); malt extract 30, mycological peptone 5, and agar 20; all ingredients were properly combined up to 1 L with distilled water and well-cooked. The inoculum of every test microorganism was prepared according to *Microbiology*, 2000 [54].

#### 2.5.3. Antimicrobial Activity Assessment for CsE and *NmE*

The agar well diffusion technique was used to investigate the ability of the crude extracts of sponges to inhibit the growth of indicator bacteria, fungi, and yeasts [55], whereas gentamycin was used as a positive antibacterial standard while, ketoconazole was a positive antifungal standard. In addition, methanol was applied as a negative control. One hundred microliters of the tested crude extracts were transferred into each inoculated well after sterilizing by ultra-filtration [21]. All plates were incubated at an

appropriate temperature for 24–48 h. After the incubation period, the radius of the clear zone around each well (Y) and the radius of the well (X) were linearly measured in mm, where dividing Y2 over X2 determines an absolute unit (AU) for the clear zone [19]. The absolute unit of crude extract, which indicates a positive result, was calculated according to the equation [56]:  $AU = Y2\pi/X2\pi$ .

### 2.6. Statistical Analysis

All statistical analyses were performed with GraphPad Prism™ version 9.1.0. (GraphPad Software Inc., San Diego, CA, USA). Statistical significance was determined using one-way ANOVA for multiple groups, followed by Tukey's test for multiple comparisons. All results were reported as the mean  $\pm$  standard deviation (SD) with significance set at  $p$  values  $\leq 0.05$ .

## 3. Results

### 3.1. Sponge Identification

The collected sponges were identified to two species (Figure 1), as follows:

- 1- Finger-sponge (*Negombata magnifica*): It is a reddish-brown, narrow, crooked branched sponge, and lives between coral reefs and rocks.
- 2- Tube-sponge (*Callyspongia siphonella*): It is a cluster of vertical tubes with a common base that lives on sheltered, hard substrate. It is smooth and has a pale purple or reddish-brown color.

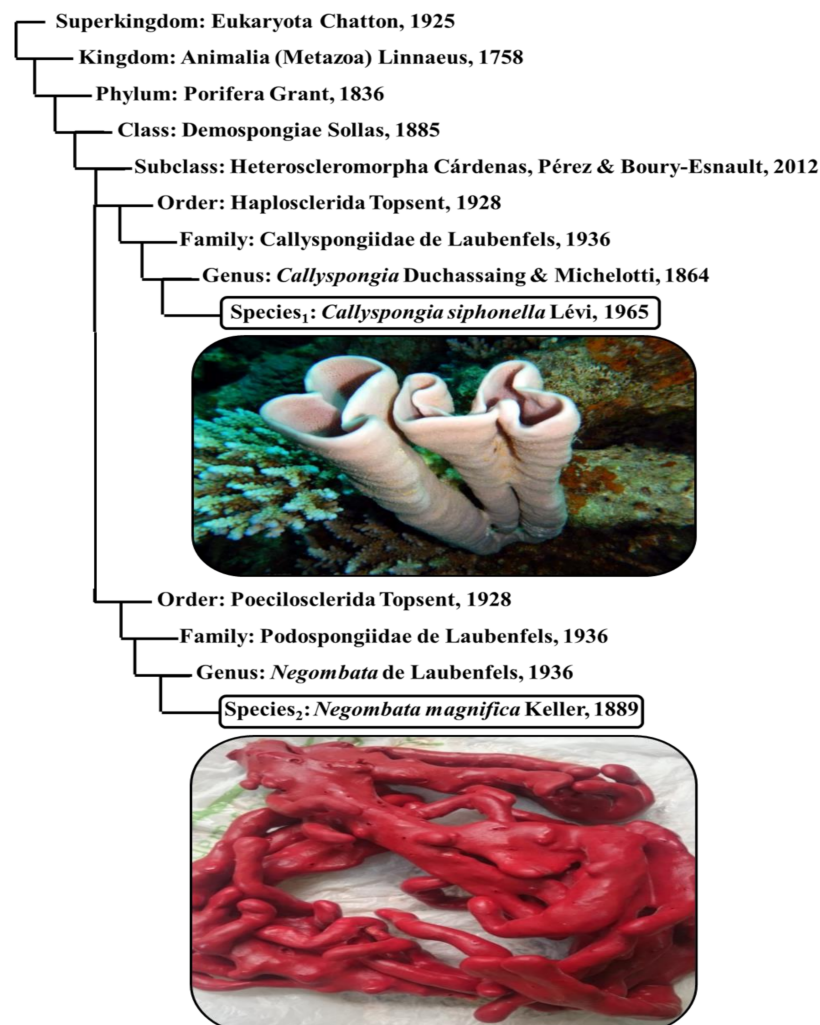


**Figure 1.** Taxonomical positions and photographs of *Callyspongia siphonella* and *Negombata magnifica*.

### 3.2. GC–MS Analysis of CsE and NmE

A total of 117 compounds have been found in both CsE and NmE, 58 for each, and 1 (10-Octadecenoic acid, methyl ester) shared. According to biological activity, 48 compounds were supposed to have biological activity (37 bioactive, 11 reported previously as a constituent for a natural organism), and 69 have no bioactivity yet. NmE has 9 compounds with anticancer activity and 6 compounds with antimicrobial activity; similarly, CsE contains 15 compounds, which have anticancer activity, 10 compounds with antimicrobial (bacteria, virus) activity, and 1 has antifungal activity (Table 1; Figures 2 and 3).

**Table 1.** Bioactive compounds of GC–MS analysis of CsE and NmE, with the reported biological activities of each compound \*.

Compound Name	Molecular Formula	RT (min)	MF	RMF	Prob (%)	CAS #	Lib	ID	MW (g/M)	Ext	Biological Activity
d-Mannose	C <sub>6</sub> H <sub>12</sub> O <sub>6</sub>	15.298	705	777	22.3%	3458-28-4	ML	37454	180	NmE	Anticancer [57] antimicrobial [58]
Cyclohexane,1-ethenyl-1-methyl-2-(1-methyleth-enyl)-4-(1-methylethylidene)-	C <sub>15</sub> H <sub>24</sub>	12.670	736	891	7.65%	3242-08-8	RL	17769	204	NmE	Anticancer [59]
γ-Elemene	C <sub>15</sub> H <sub>24</sub>	12.670	748	944	11.5%	29873-99-2	ML, RL	91836	204	NmE	Antimicrobial [60]
β-Guaiene	C <sub>15</sub> H <sub>24</sub>	15.956	701	763	6.59%	88-84-6	ML	133155	204	NmE	Antimicrobial [61]
(-)-Spathulenol	C <sub>15</sub> H <sub>24</sub> O	18.751	776	813	10.1%	77171-55-2	ML	5991	220	NmE	Antiproliferative [62]
Isoaromadendrene epoxide	C <sub>15</sub> H <sub>24</sub> O	18.751	780	841	11.9%	N/A	ML	2203	220	NmE	Anticancer [63]
Undecanoic acid, 11-bromo-, methyl ester	C <sub>12</sub> H <sub>23</sub> BrO <sub>2</sub>	17.336	666	715	4.16%	6287-90-7	RL	9817	278	NmE	Antimicrobial [64]
Desulphosinigrin	C <sub>10</sub> H <sub>17</sub> NO <sub>6</sub> S	15.725	704,	776	27.4%	5115-81-1	ML	28432	279	NmE	Anticancer [65]
Androstan-17-one, 3-ethyl-3-hydroxy-, (5α)-	C <sub>21</sub> H <sub>34</sub> O <sub>2</sub>	18.751	722	746	5.12%	57344-99-7	ML	55206	318	NmE	Antimicrobial [66]
Propanoic acid, 2-methyl-,(dodecahydro-6a-hydroxy-9a-methyl-3-methylene-2,9-dioxoazuleno [4,5-b]furan-6-yl)m	C <sub>19</sub> H <sub>26</sub> O <sub>6</sub>	16.609	699	733	4.32%	33649-17-1	ML	7019	350	NmE	Anticancer [67]
9,10-Secochole-5,7,10(19)-trien-24-al, 3-hydroxy-, (3.β.,5Z,7E)-	C <sub>24</sub> H <sub>36</sub> O <sub>2</sub>	16.609	723	804	10.5%	40013-88-5	ML	88071	356	NmE	Anticancer [68]
Mannofuranoside	C <sub>21</sub> H <sub>36</sub> O <sub>6</sub>	15.956	693	745	4.70%	N/A	ML	31505	384	NmE	Anticancer [69]
Docosahexaenoic acid	C <sub>25</sub> H <sub>40</sub> O <sub>2</sub> Si	15.500	645	658	8.94%	N/A	ML	37920	400	NmE	Anticancer [70]

Table 1. Cont.

Compound Name	Molecular Formula	RT (min)	MF	RMF	Prob (%)	CAS #	Lib	ID	MW (g/M)	Ext	Biological Activity
Digitoxin	C <sub>41</sub> H <sub>64</sub> O <sub>13</sub>	13.351	603	641	9.74%	71-63-6	RL	8938	764	NmE	Antiviral [71], anticancer [72]
2-Tridecanone	C <sub>13</sub> H <sub>26</sub> O	20.455	746	827	5.68%	593-08-8	RL	6452	198	CsE	Antimicrobial [73]
2-Pentadecanone	C <sub>15</sub> H <sub>30</sub> O	20.455	752	834	7.22%	2345-28-0	ML	25959	226	CsE	Anticancer [74]
tert-Hexadecanethiol	C <sub>16</sub> H <sub>34</sub> S	29.303	711	761	10.7%	25360-09-2	ML	23376	258	CsE	Anticancer [75]
9,12-Octadecadienoic acid (Z,Z)-	C <sub>18</sub> H <sub>32</sub> O <sub>2</sub>	37.203	709	751	3.03%	60-33-3	RL	7667	280	CsE	Anticancer [74]
2-Nonadecanone	C <sub>19</sub> H <sub>38</sub> O	20.455	771	906	14.2%	629-66-3	ML	25712	282	CsE	Anticancer [76]
cis-Vaccenic acid	C <sub>18</sub> H <sub>34</sub> O <sub>2</sub>	25.353	763	791	5.10%	506-17-2	ML	18782	282	CsE	Antimicrobial [77]
trans-13-Octadecenoic acid	C <sub>18</sub> H <sub>34</sub> O <sub>2</sub>	25.353	760	792	4.53%	693-71-0	ML	18062	282	CsE	Antimicrobial [78]
Hexadecanoic acid, ethyl ester	C <sub>18</sub> H <sub>36</sub> O <sub>2</sub>	22.095	789	812	17.2%	628-97-7	ML, RL	52733	284	CsE	Antibacterial [79]
Octadecanoic acid, ethyl ester	C <sub>20</sub> H <sub>40</sub> O <sub>2</sub>	22.095	778	834	8.68%	111-61-5	RL	12005	312	CsE	Anticancer [80]
Octadecane, 3-ethyl-5-(2-ethylbutyl)-	C <sub>26</sub> H <sub>54</sub>	44.128	681	686	3.65%	55282-12-7	ML	7471	366	CsE	Antibacterial [81]
Fenretinide	C <sub>26</sub> H <sub>33</sub> NO <sub>2</sub>	53.432	655	713	6.97%	65646-68-6	ML	77816	391	CsE	Antiviral (anti-COVID-19) [11] and anticancer [82]
Ursodeoxycholic acid	C <sub>24</sub> H <sub>40</sub> O <sub>4</sub>	44.128	668	680	3.63%	128-13-2	ML	19201	392	CsE	Anticancer [83]
Campesterol	C <sub>28</sub> H <sub>48</sub> O	47.068	726	776	14.8%	474-62-4	ML	6713	400	CsE	Anticancer [84]
Ergost	C <sub>28</sub> H <sub>48</sub> O	47.068	680	821	1.92%	4651-51-8	ML	6865	400	CsE	Anticancer [85]
25-Hydroxycholesterol	C <sub>27</sub> H <sub>46</sub> O <sub>2</sub>	44.128	670	703	5.61%	2140-46-7	ML	27474	402	CsE	Anti-viral [86] anticancer [87]
Stigmasterol	C <sub>29</sub> H <sub>48</sub> O	44.128	683	730	8.43%	83-48-7	RL, ML	19475	412	CsE	Anticancer [88], antibiotic [89]
β-Sitosterol	C <sub>29</sub> H <sub>50</sub> O	47.068	743	777	27.6%	83-46-5	RL	1982	414	CsE	Anticancer [90]
γ-Sitosterol	C <sub>29</sub> H <sub>50</sub> O	47.068	738	752	22.2%	83-47-6	ML	6839	414	CsE	Anticancer [91]
Ethyl iso-allocholate	C <sub>26</sub> H <sub>44</sub> O <sub>5</sub>	40.316	658	666	4.38%	N/A	ML	6654	436	CsE	Anticancer [92] and antiviral (anti-COVID-19) [11]
Retinoyl-β-glucuronide	C <sub>26</sub> H <sub>34</sub> O <sub>7</sub>	51.087	614	654	6.30%	101470-87-5	ML	132135	458	CsE	Antibacterial [93]

**Table 1.** Cont.

Oleic acid, eicosyl ester	C <sub>38</sub> H <sub>74</sub> O <sub>2</sub>	34.443	656	665	2.87%	22393-88-0	ML	25265	562	CsE	Cancer preventive [94,95]
Oleic acid, 3-(octadecyl-oxy)propyl ester	C <sub>39</sub> H <sub>76</sub> O <sub>3</sub>	34.443	657	689	2.99%	17367-41-8	ML	22460	592	CsE	Antifungal [96]

\* CAS #, Chemical abstract service registry number; Ext, Extract; ID, Identification number; Lib, Library type; MF, Match factor; ML, Main library; MW, Molecular weight; N/A, Not available; Prob, Probability; RL, Reliable library; RMF, Reverse match factor; RT, Retention time. Relative abundance.

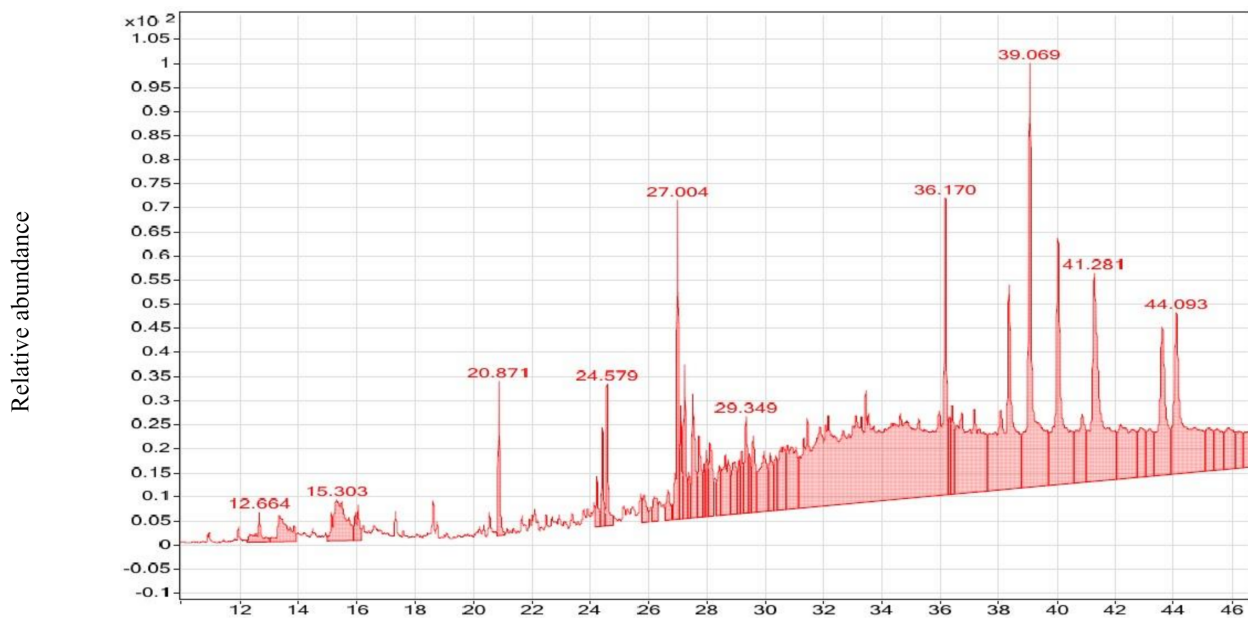


**Figure 2.** GC-MS chromatogram of NmE.

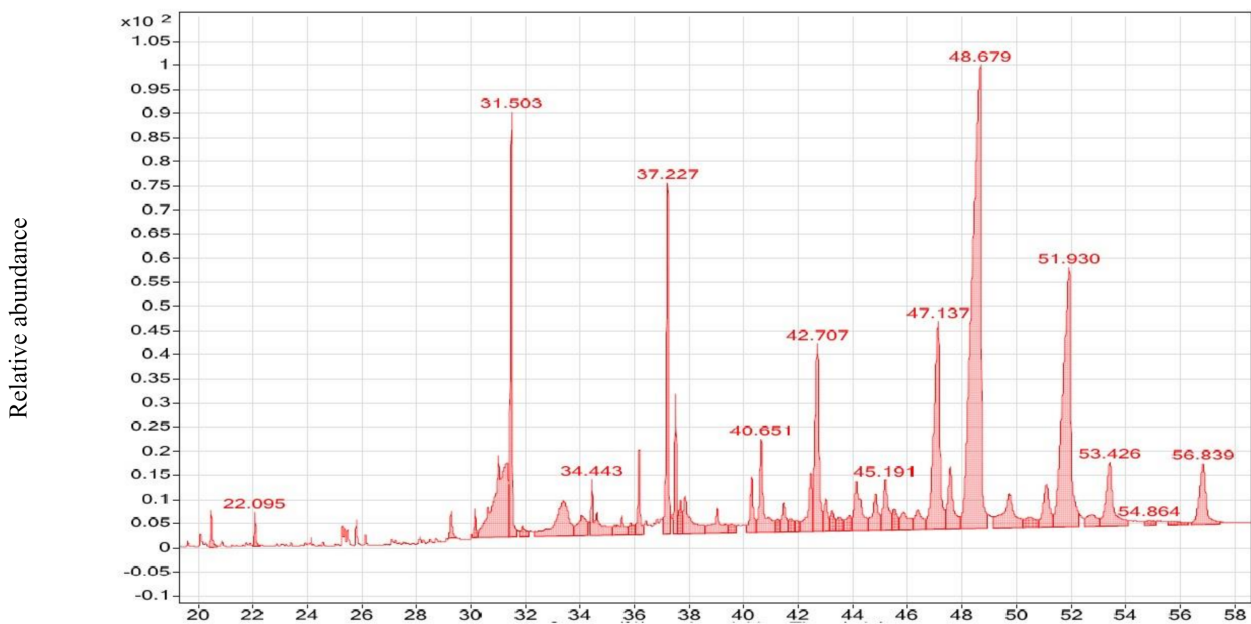


**Figure 3.** GC-MS chromatogram of CsE.

### 3.3. Anticancer Effects of CsE and NmE

#### 3.3.1. CsE and NmE Effects on HepG2, MCF-7, and Caco-2 Cells Proliferation and Viability

Both extracts inhibited the growth of all investigated cancer cells in different dose-dependent manners with remarkable decrease in cell viability (Figures 4 and 5) associated with cytotoxicity increase. The  $IC_{50}$  values between NmE and CsE are greatly different indicating the higher efficacy of NmE in the inhibition of HepG2, MCF-7, and Caco-2 cancer cells proliferation. The  $IC_{50}$  values for NmE and CsE on HepG2 cells were 10.33 and 271.48  $\mu\text{g/mL}$ , respectively, while on MCF-7, they were 12.48 and 467.19  $\mu\text{g/mL}$ , respectively, whereas on Caco-2, cells were 10.52 and 1570.82  $\mu\text{g/mL}$ , respectively (Table 2). Due to the NmE potentiality as an antiproliferative active agent, it was chosen for further investigations.

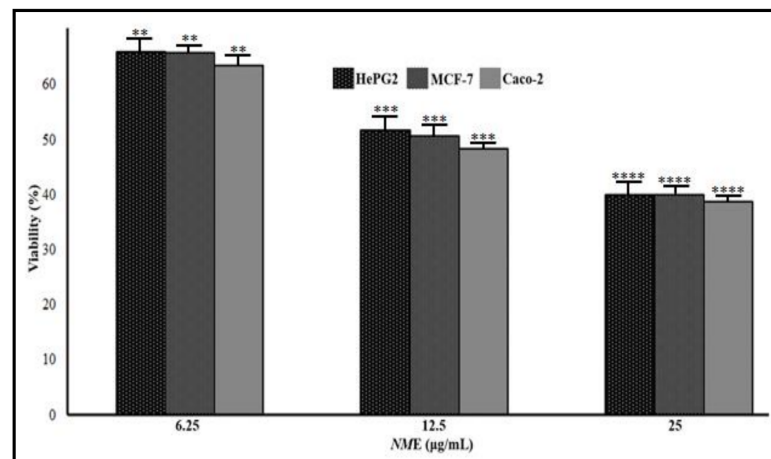


**Figure 4.** Effects of NmE on HepG2, MCF-7, and Caco-2 cell viability after 48 h. Cells were incubated with the indicated concentration of NmE while the percentage of cell viabilities were determined by MTT. Values used for plotting are means of triplicates, with each concentration tested in 7–8 wells. Statistical differences from control cultures are shown as bar graphs with error bars representing the means  $\pm$  SD; \*\*  $p < 0.01$ , \*\*\*  $p < 0.001$  and \*\*\*\*  $p < 0.0001$  vs. control (DMSO-treated) cells.

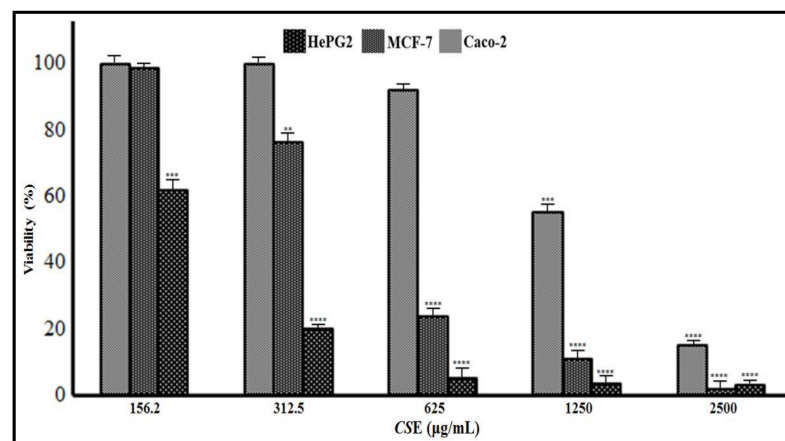


**Figure 5.** Effects of CsE on HepG2, MCF-7, and Caco-2 cell viability after 48 h. Cells were incubated with the indicated concentration of CsE while the percentage of cell viabilities were determined by MTT. Values used for plotting are means of triplicates, with each concentration tested in 7–8 wells. Statistical differences from control cultures are shown as bar graphs with error bars representing the means  $\pm$  SD; \*\*  $p < 0.01$ , \*\*\*  $p < 0.001$  and \*\*\*\*  $p < 0.0001$  vs. control (DMSO-treated) cells.

**Table 2.** The IC<sub>50</sub> values (µg/mL) for *NmE* and *CsE* on HepG2 cells.

Investigated Cancer Cells	Investigated Extract	
	<i>NmE</i>	<i>CsE</i>
HepG2	10.33	271.48
MCF-7	12.48	467.19
Caco-2	10.52	1570.82

### 3.3.2. *NmE* Induced Apoptosis and Increased Bax, Cleavage PARP, and Caspase-3 Expressions in Cancer Cells

In HepG2, *NmE* in a dose-dependent manner induced significant early and late apoptosis causing complete cell death (Figures 6 and 7), indicated by the elevated percentage of PI stain that binds to the genetic material (DNA and RNA) inside the damaged dead cells. In addition, the *NmE* apoptotic effect is confirmed through the expression of some regulatory proteins that are involved in either the extrinsic or intrinsic apoptotic pathways. *NmE* increased the level of the pro-apoptotic protein Bax, cleavage PARP, and caspase-3, while it decreased the level of the anti-apoptotic protein BCL2 in HepG2, MCF-7, and Caco-2 cancer cell lines (Figure 8).

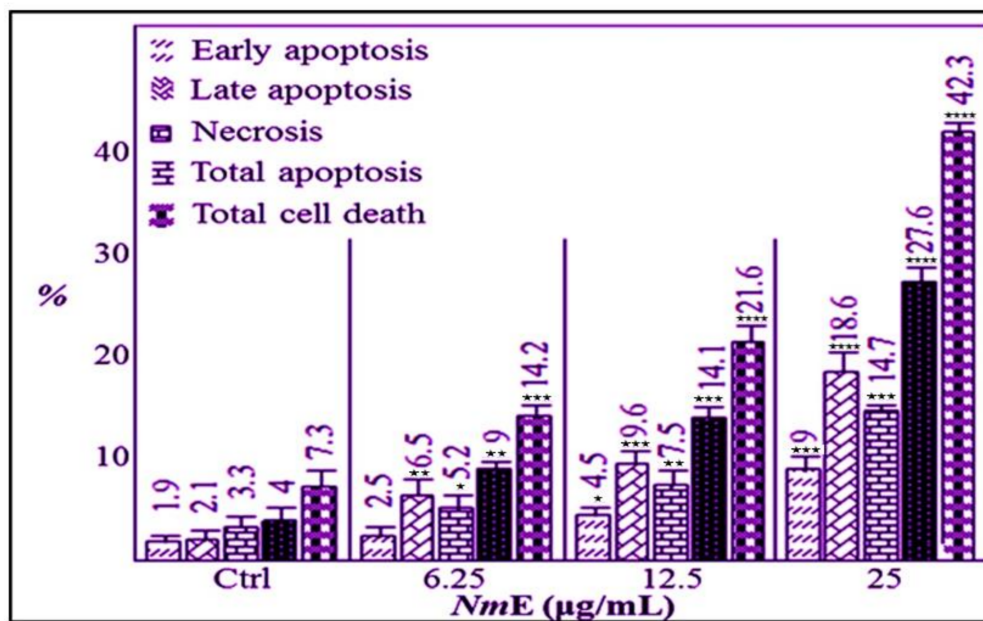


**Figure 6.** Percentages of apoptosis, necrosis, and cell death induced by *NmE* in HepG2 cells. Bars represent the means  $\pm$  SD. \*  $p < 0.05$ , \*\*  $p < 0.01$ , \*\*\*  $p < 0.001$  and \*\*\*\*  $p < 0.0001$  vs. control (DMSO-treated) cells.

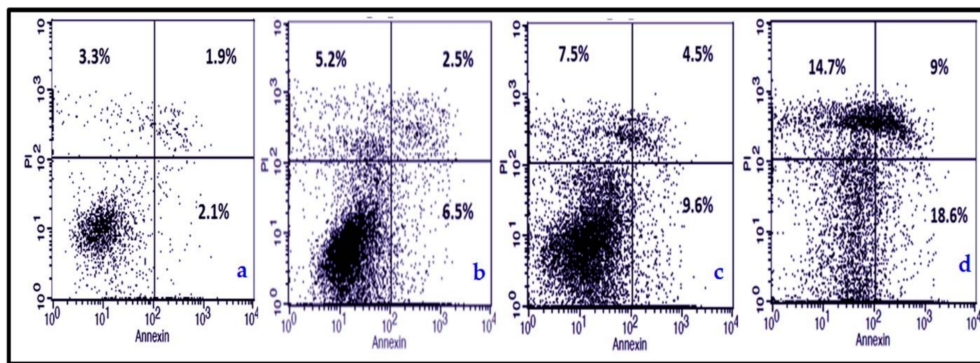


**Figure 7.** Cell death percentage induced by *NmE* in HepG2 cells: (a) Ctrl. HepG2, (b) *NmE* (6.25  $\mu\text{g/mL}$ )/HepG2, (c) *NmE* (12.5  $\mu\text{g/mL}$ )/HepG2, and (d) *NmE* (25  $\mu\text{g/mL}$ )/HepG2.

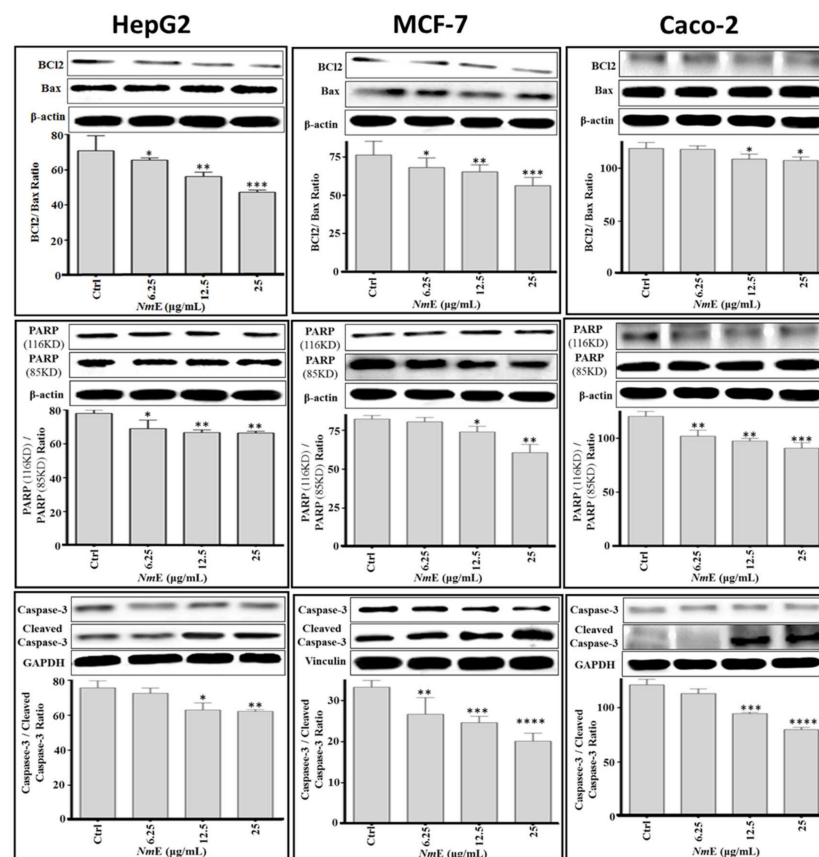


**Figure 8.** Effects of *NmE* on protein expression of BCL2, Bax, cleaved PARP, and cleaved Caspase-3 in HepG2, MCF-7, and Caco-2 cells, which were treated with each *NmE* concentration and harvested 48 h after treatments. The immunoblots shown are representative of three independent experiments, which all gave similar results, cropped and unedited images are provided here. Bars represent the means  $\pm$  SD. \*  $p < 0.05$ , \*\*  $p < 0.01$ , \*\*\*  $p < 0.001$  and \*\*\*\*  $p < 0.0001$  vs. control (DMSO-treated) cells.

### 3.3.3. *NmE* Induced G0/G1-Phase Cell Cycle Arrest and Decreased Cyclins D1 and E1 and CDK6 Expressions in Cancer Cells

The cell cycle profile analysis revealed significant dose-dependent increases in the number of cells in the G0/G1 phase of the cell cycle in *NmE*-exposed HepG2 cells compared to no-treatment HepG2 cells control (Figures 9 and 10). The G0/G1 phase distribution of HepG2 cells after treatment with *NmE* (0, 6.25, 12.5, and 25  $\mu\text{g/mL}$ ) was 45.8%, 49.83%, 59.67%, and 67.56%, respectively (Figure 10). The increases in the G0/G1 phase cell population were accompanied by decreases in the G2/M and S phase cell populations of

the HepG2 cell line except for a slight increase for the S phase at the 25 µg/mL dose of *NmE*. This slight increase in the S phase at this highest dose of *NmE* (25 µg/mL) is suggestive as evidence of toxicity. Since the current cell cycle analysis elucidated that *NmE* treatment of HepG2 cells resulted in a G0/G1-phase arrest, we next assessed the effect of *NmE* on cell cycle regulatory proteins that are effective in the G1 phase. Thus, we examined the effect of *NmE* on the expression of cyclins D1 and E1 and CDK6. *NmE* showed a dose-dependent decrease in the expression of cyclins D1 and E1 and CDK6 (Figure 11) in HepG2, MCF-7, and Caco-2 cancer cell lines. To conclude, *NmE*-induced cell cycle arrest is mediated via inhibiting CDK6 along with cyclins D1 and E1.

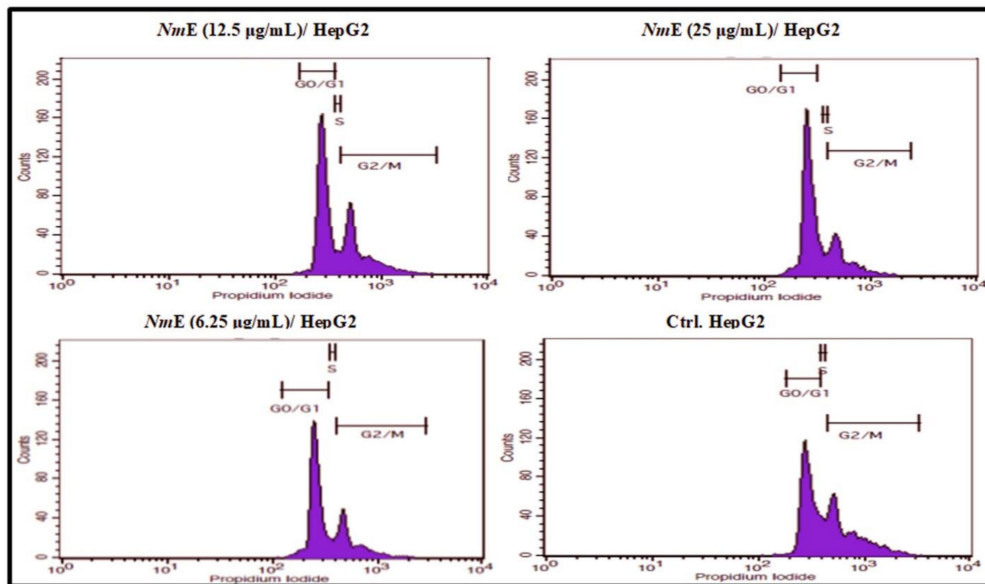


Figure 9. Cell cycle analysis of HepG2 cell line treated with *NmE*.

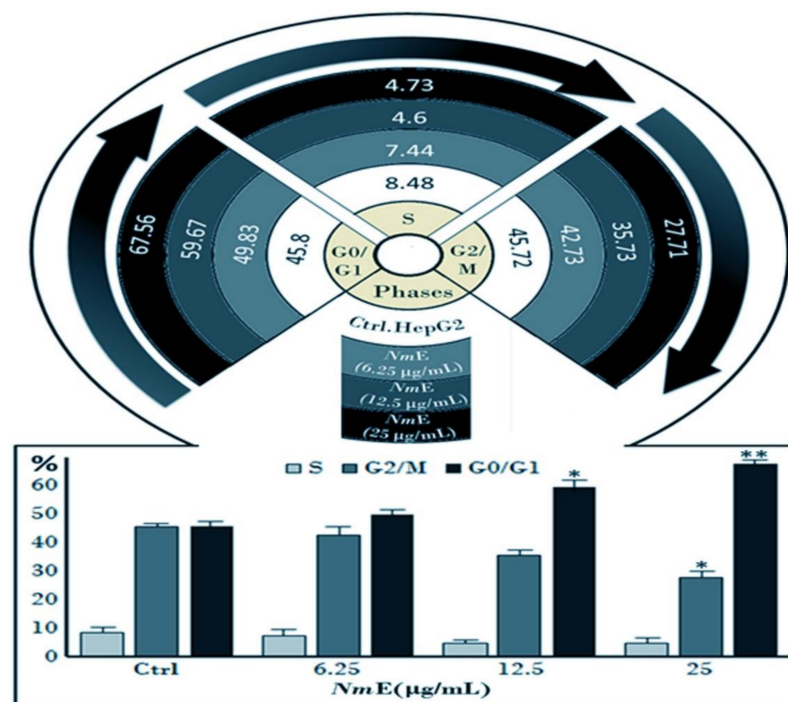
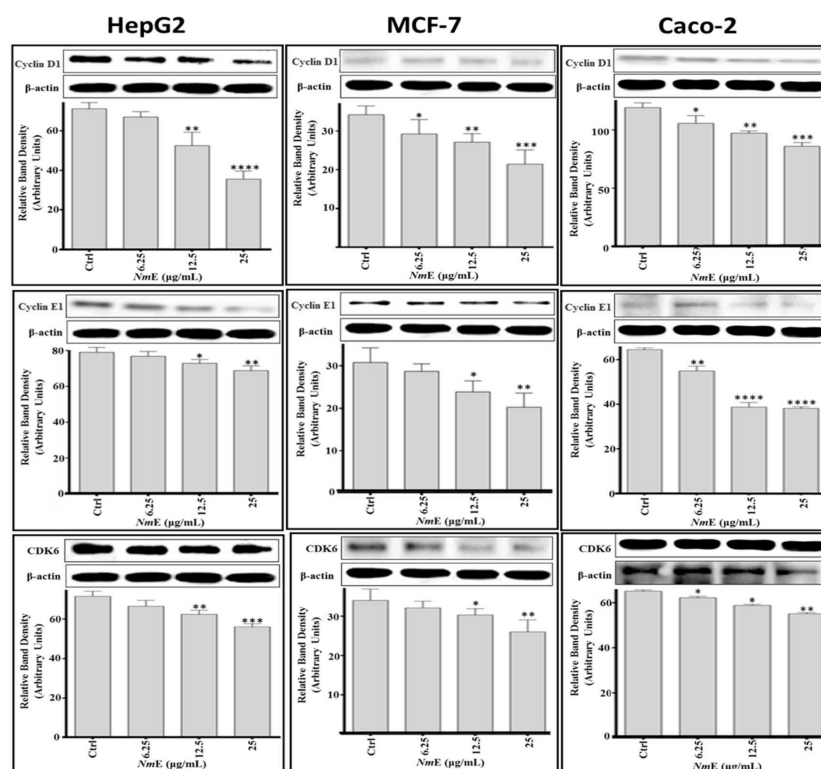


Figure 10. Schematic drawing and bar chart for the cell cycle analysis expressed by (%) of HepG2 cells in each phase when treated with *NmE*. Bars represent the means ± SD. \*  $p < 0.05$  and \*\*  $p < 0.01$ , vs. control (DMSO-treated) cells.



**Figure 11.** Effects of *NmE* on protein expression of Cyclin D1, Cyclin E1, and in HepG2, MCF-7, and Caco-2 cancer cells, which were treated with each *NmE* concentration and harvested 48 h after treatments. The immunoblots shown are representative of three independent experiments, which all gave similar results, only representative, cropped, and unedited images are provided here. Bars represent the means  $\pm$  SD. \*  $p < 0.05$ , \*\*  $p < 0.01$ , \*\*\*  $p < 0.001$  and \*\*\*\*  $p < 0.0001$  vs. control (DMSO-treated) cells.

### 3.3.4. *NmE* Triggered ROS Production in HepG2 Cell Line

The current flowcytometric analysis showed that *NmE*-treated HepG2 cells produced more ROS compared to untreated HepG2 cells (Figure 12). *NmE* was able to increase the ROS production, even the *NmE* lower concentration (6.25  $\mu\text{g}/\text{mL}$ ) was significant to induce higher ROS production than HepG2 cells control. In summary, it seems that *NmE* produced marked induction of apoptosis and anti-proliferative activity on HepG2, MCF-7, and Caco-2 cancer cells via multiple pathways (Figure 13).

### 3.4. Antimicrobial Activity of CsE and *NmE*

The results showed a noticeable antimicrobial activity against a wide range of the test organisms (Table 3). CsE was effectively more than *NmE* against *Aspergillus flavus*, *Cryptococcus neoformans*, *Salmonella typhimurium*, *Klebsiella pneumonia*, *Streptococcus mutants*, and *Candida lipolytica*, while *NmE* showed positive antibacterial activity against *Escherichia coli* and MRSA. The most susceptible test organism is *Salmonella typhimurium* followed by *Streptococcus mutants*. The most resistant strain is *Penicillium expansum*. While CsE could not affect the growth of *Escherichia coli* and MRSA, the *NmE* did.

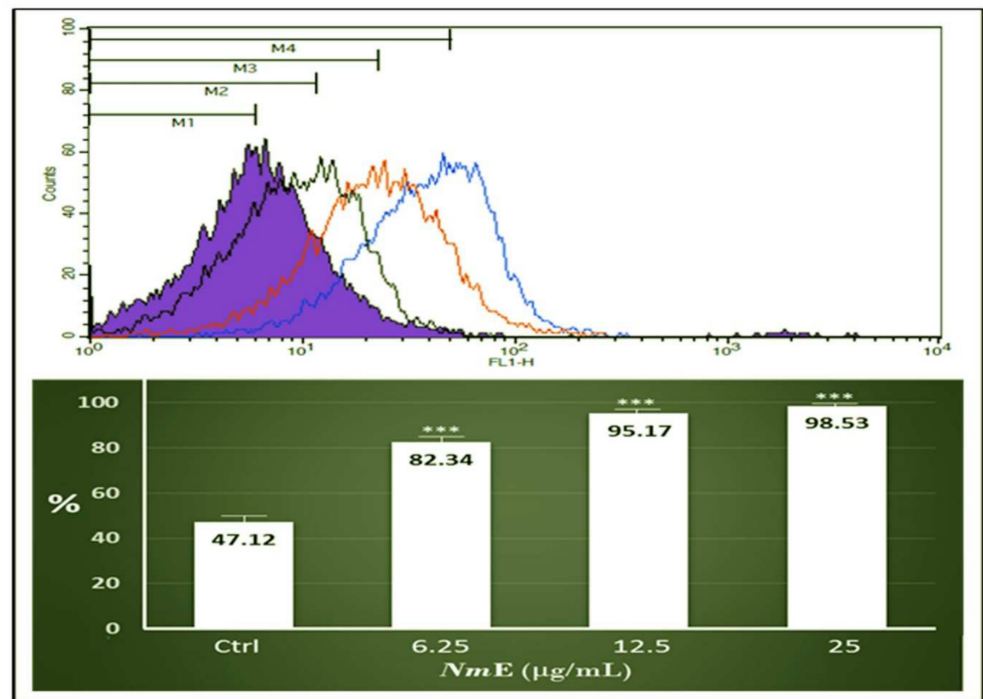


**Figure 12.** Effects of *NmE* on ROS production in HepG2 cancer cells. The maximum effect occurred at 48 h post-treatment. Bars represent the means  $\pm$  SD. \*\*\*  $p < 0.001$  vs. control (DMSO-treated) cells.

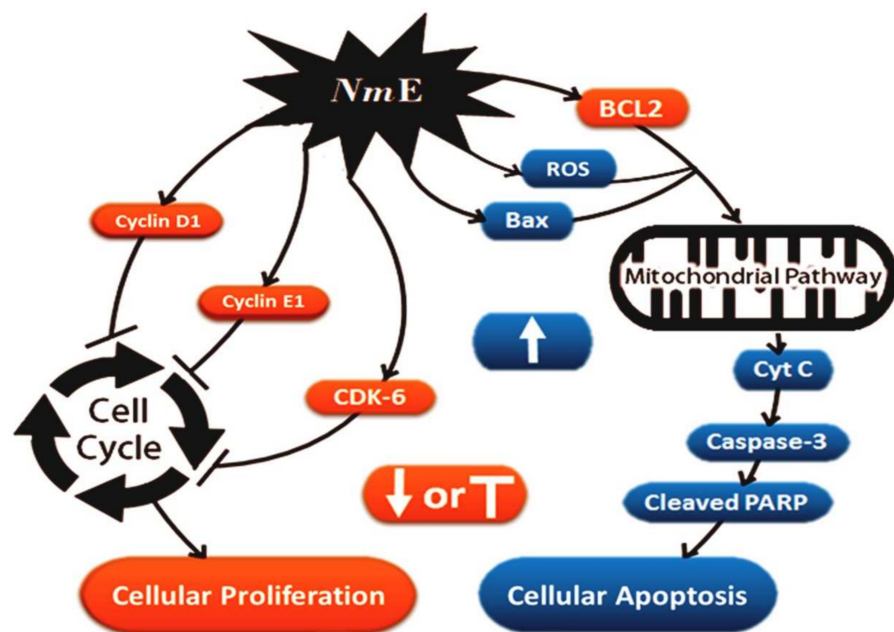


**Figure 13.** Schematic drawing of the mechanism of action of *NmE*. This cartoon is based on the current available data throughout 474 the present study.

**Table 3.** Antimicrobial activity of CsE and NmE.

Tested Microorganisms		AU by the Crude Extracts		Positive Standard
		CsE	NmE	
Fungi * Ketoconazole 100 µg	<i>Aspergillus flavus</i>	2.42	-ve	3.16
	<i>Penicillium expansum</i>	-ve	-ve	2.42
	<i>Candida lipolytica</i>	2.78	-ve	4.0
	<i>Cryptococcus neoformans</i>	2.09	-ve	2.42
Gram-negative bacteria * gentamycin 4 µg	<i>Escherichia coli</i>	-ve	2.42	4.46
	<i>Salmonella typhimurium</i>	4.46	-ve	3.57
	<i>Klebsiella pneumonia</i>	2.09	-ve	-
Gram-positive bacteria * gentamycin 4 µg	<i>Micrococcus</i> sp.	-ve	-ve	5.98
	<i>Streptococcus mutants</i>	3.16	-ve	4.94
	MRSA	-ve	3.57	11.11

Data expressed as AU ranged from 2.09 to 4.46 for the sponge extracts in corresponding to the AU resulted by positive control, which ranged from 2.42 to 11.11. \* Positive standard

All the values resulting from the sponge crude extracts are lower than those obtained by the positive standard; however, it was noticed that CsE had an antibacterial potential against *Klebsiella pneumonia* while, ketoconazole as a positive control, had no antibacterial activity against this strain so, this is a very promising result.

Entirely, with a careful look at Table 3, it is observed that CsE has a superior antifungal rather than antibacterial activity, and therefore might be classified as a moderate potent antifungal agent and as a mild to moderate antibacterial, and vice versa with NmE, which has only a limited antibacterial activity, and therefore might be classified as weak to a mild antibacterial agent.

#### 4. Discussion

Bioactive chemicals generated from marine sponges are well-known for their pharmacodynamic potential in the treatment of a variety of disorders. The current high anticancer effect of NmE may be attributable to the fact that it contains nine anticancer chemicals (see Table 1) that triggered apoptosis and suppressed proliferation in cancer cell lines HepG2, MCF-7, and Caco-2. According to the present findings, NmE inhibited the growth of HepG2, MCF-7, and Caco-2 cancer cells dose-dependently with IC50 values of 10.33, 12.48, and 10.52 g/mL, respectively, and induced apoptosis in HepG2, MCF-7, and Caco-2 cells by increasing pro-apoptotic proteins Bax, caspase-3, and cleavage PARP, and decreasing anti-apoptotic protein BCL2. Rady and Bashar [1] confirmed the different extracts (methylene chloride, ethyl acetate, acetone, and chloroform) of *Negombata magnifica* have induced antiproliferation activity against HepG2 cancer cell line within IC50 values 9.14, 10.94, 8.78, and 7.23 µg/mL, respectively; MCF-7 cancer cell lines within IC50 values of 7.65, 6.18, 11.82, and 8.26 µg/mL, respectively; and Caco-2 cancer cells within IC50 values of 12.67, 9.27, 8.37, and 10.68 µg/mL, respectively, as well as the same extracts induced apoptosis in HepG2, MCF-7, and Caco-2 cancer cell lines through Bax and caspase-3 increase and BCL2 decrease. The ethanolic extract of *Negombata magnifica* induced intense anticancer activities against Caco-2 and MCF-7 cancer cells with lower values of IC50 (1.09 and 0.37 g/mL, respectively) [19], while the differences in values of IC50 overall indicated that all *N. magnifica* extracts are highly potential for anticancer properties. However, more research into the effects of the ethanolic extract on the cancer cell cycle and cancer cell-induced apoptosis is needed.

Similarly, CsE present modest anticancer activity could be linked to its GC-Mass study, which revealed that it contains 15 anticancer chemicals (Table 1). In the same context, El-Hawary et al. [39] discovered that the ethanol crude extract of *Callyspongia siphonella* has antiproliferative action against the MM.1S, OVCAR-3, and HT-29 cancer cells. Moreover, dehydroisophonochalynol and Callyspongenols were extracted from the organic extract of *Callyspongia fistularis* and showed cytotoxic activities against HeLa and P388 cancer

cells [41]. On the other side, Rady and Bashar [1] stated that the different extracts of *C. siphonella* potentially inhibited the growth of Caco-2, MCF-7, and HepG2 cells with IC<sub>50</sub> values lower than that recorded in the present methanolic extract, as well as inducing apoptosis in Caco-2, MCF-7, and HepG2 cells through an increase in Bax and caspase-3 along with a decrease in BCL2. Ibrahim et al. [21] found the ethanolic extract of *C. siphonella* was more efficient as an anticancer agent against MCF-7 and Caco-2 cancer cells, than the current methanolic one.

Although each of the current CsE and NmE concentrations was found to inhibit cell proliferation in Caco-2, MCF-7, and HepG2 cancer cells in vitro, only three NmE concentrations (6.25, 12.5, and 25 g/mL) were used in the treatment of Caco-2, MCF-7, and HepG2 cancer cells, whereas five CsE concentrations (156.2, 312.5, 625, 1250, and 2500 µg/mL) were used. As previously stated, the highest concentration of CsE was 100 times that of NmE, which may explain the significant variation in the values of IC<sub>50</sub> for the two extracts for their cell proliferation inhibition properties in HepG2, MCF-7, and Caco-2 cancer cells, where the values of IC<sub>50</sub> for CsE (271.48, 467.19, and 1570.82 g/mL), respectively, were significantly higher than that of NmE (10.33, 12.48, and 10.52 µg/mL), respectively. Therefore, in the current investigation, NmE was chosen to undertake further anticancer screening methods, which revealed more about NmE anticancer efficacy in HepG2, MCF-7, and Caco-2 cancer cells. In HepG2, MCF-7, and Caco-2 cancer cells; however, the in vitro anticancer effects of NmE were supported by a decrease in CDK6, BCL2, and cyclins E1 and D1, as well as an increase in Bax, cleaved PARP, and caspase-3; in addition, the anticancer effects of other previously researched bioactive chemicals of marine species resulted in BCL2, STAT3, and MMP-9 decreases in HepG2 cancer cell line, in addition to the stimulation of G0/G1 cell cycle arrest and ROS buildup [97]. Furthermore, a study using quantitative real-time PCR analysis revealed that the administration of cerebrosides from *Asterias amurensis* or *Acaudina molpadioides* decreased BCL2 and Bcl-xL expression while increasing caspase-3, Cyt c, Bax, and caspase-9 expression in the murine sarcoma cell line-180 ascites [98,99]; unlike another in vivo investigation that indicated philinopside E anti-angiogenic activity correlated with the downturn of VEGFR2 signaling in murine sarcoma cancer cells, the current NmE was studied in vitro where it suppressed the expression of BCL2 and increased the expression of cleaved PARP, Bax, and caspase-3 in MCF-7, HepG2, and Caco-2 cancer cell lines. Even though clinical study on the anticancer efficacy of bioactive components from marine sources is highly limited, there is one study in which TBL12 was given to 20 patients with high-risk asymptomatic multiple myeloma. TBL12 was well tolerated, and 9 (45%) of the patients are still on treatment with only one minimal response [100].

As a result, the current potent CsE antibacterial activities can be attributed to its GC-Mass analysis, which contains five antimicrobial molecules. The *Callyspongia siphonella* methanol extract within its antibacterial components explains antimicrobial activities against *Streptococcus* mutants, *Klebsiella pneumonia*, and *Salmonella typhimurium*, in comparison to the antimicrobial activities of another ethanolic extract of the same sponge, including its two brominated oxindole alkaloids bioactive substances, which undoubtedly played a crucial part in robust antibacterial activity against Gram-positive bacteria, *Bacillus subtilis* and *Staphylococcus aureus*, as well as moderate biofilm inhibitory action against *Pseudomonas aeruginosa* [39]. Furthermore, when compared to methanolic extract of *Callyspongia reticulata*, which showed less antibacterial activities in a specific fungicidal against *Candida albicans*, *Penicillium notatum*, and *Aspergillus niger* [101], the present CsE had a wider and more effective antimicrobial activity toward *Cryptococcus neoformans*, *Klebsiella pneumonia*, *Salmonella typhimurium*, *Aspergillus flavus*, *Candida* spp., and *Streptococcus* mutants. Like the antimicrobial activity of CsE, the sponges *Ircinia strobilina*, *Ircinia felix*, and *Acanthella carteri* displayed wide-spectrum antimicrobial activity toward *Candida tropicalis*, *C. albicans*, *Bacillus subtilis*, *Proteus vulgaris*, *Escherichia coli*, and *Staphylococcus aureus* [102].

Emerging bacterial resistance leads to finding new advanced antibacterial agents [103] specifically those that belong to the natural origin starting from the microorganisms [104,105],

plants [55], and other living forms. So, the present moderate *NmE* antibacterial properties can be attributed to the GC-Mass analysis of it, which contains only four antimicrobial substances as explained in Table 1. In addition, two compounds might have antimicrobial activity:  $\beta$ -Guaiene has been reported as an essential oil extract constituent [61]; and androstan-17-one, 3-ethyl-3-hydroxy-, (5 $\alpha$ ) has been reported as an *Araucaria cunninghamii* methanol extract constituent [66]. The current *NmE* induced positive antibacterial activity against *Escherichia coli* and MRSA, whereas the ethanol extract of *Negombata magnifica* [19] and the methanol extract of *Negombata cortica* [102] had no antimicrobial activity.

Some of the current GC-Mass compounds have additional bioactivity besides their anticancer or antimicrobial activity, for instance, fenretinide and ethyl iso-allocholate, which had anti-COVID-19 activity [11,12]. Although the current investigation assessed the anticancer and antimicrobial activity of *NmE* and *CsE*, there are about eighty-one chemical compounds in the present GC-Mass analysis for both *NmE* and *CsE* that have not yet revealed any anticancer or antimicrobial properties, and they will require more research to demonstrate their anticancer or antimicrobial activity. Sixty-nine of those chemical compounds have no reports for their biological activity, e.g., ethyl 9,12-hexadecadienoate and 2-heptadecanone, while the other 12 compounds are biologically active, such as desoximetasonone, which has shown anti-psoriasis activity [106,107], and ergosta-5,22, which has demonstrated anti-inflammatory activity [108].

In the end, we conclude that because of the worrisome increase in the incidence of cancer and other emerging microbes or viruses, such as SARS-CoV-2, humanity needs to procedure many studies directed towards finding promising solutions to overcome these stubborn diseases. Though chemotherapy is an effective way to treat many types of cancer, chemotherapy treatment carries a risk of side effects. Some chemotherapy side effects are mild and treatable, while others can cause serious complications. Therefore, the trend now is to return to nature to discover more natural remedies that contain natural chemicals, which do not have, or have few, side effects. The marine ecosystem is rich in its components that are characterized as diverse in their species and benefits, which vary from the unseen microorganisms to huge macroorganisms [109–112].

## 5. Conclusions

To our knowledge, the present study represents the first assessment of *NmE* influence on the cancer cell (HepG2) cycle profile analysis, and ROS production, of the antimicrobial activity of both *CsE* and *NmE*. The data generated during the current study emphasize our hypothesis, namely, that *NmE* has anti-cancer properties that might be promising, and can be developed in the future as an anti-cancer drug for cancer therapy outcomes, and also that *CsE* acts as a vital source for antimicrobial drug discovery. Therefore, the findings in this study recommend increasing research in this field, which can have solutions in treating many intractable diseases.

**Author Contributions:** I.R., M.S.E.-W., W.B.S., F.O.A.-O., S.A.A.-R., L.M.A.E.-M. and E.M.H.A. performed the experiments. H.A.E.-N. and E.-S.S.S. collected sponge specimens from Red Sea via SCUBA diving. H.A.E.-N. and W.B.S. conceived, designed, and supervised the study, and provided key insights into the planning of the project, interpretation of the data, revised the final manuscript for intellectual content and coordinated the study, as well as all other authors. H.A.E.-N., M.A.E.B., I.R., and W.B.S. analyzed the data and wrote the first draft of the manuscript. F.O.A.-O. and S.A.A.-R. Contributed reagents, materials, laboratory, and grant support for the project. S.B. and design the study, validation, supervision and revised the final manuscript for intellectual content and coordinated the study. All authors have read and agreed to the published version of the manuscript.

**Funding:** This research project was supported by a grant from the Researchers Supporting Project number (RSP2021/114), King Saud University, Riyadh, Saudi Arabia.

**Institutional Review Board Statement:** Not applicable.

**Informed Consent Statement:** Not applicable.

**Data Availability Statement:** The datasets generated during and/or analyzed through the current study are available from all authors.

**Acknowledgments:** The authors would like to extend their sincere appreciation to the Research Supporting Project number: RSP-2021/114, King Saud University, Riyadh, Saudi Arabia.

**Conflicts of Interest:** The authors declare no conflict of interest.

## References

1. Rady, I.; Bashar, M.A.E. Novel extracts from *Callyspongia siphonella* and *Negombata magnifica* sponges from the Red Sea, induced antiproliferative and proapoptotic activity in HepG-2, MCF-7, and Caco-2 cancer cell lines. *Egypt. J. Aquat. Biol. Fish.* **2020**, *24*, 319–347. [[CrossRef](#)]
2. Metwally, A.S.; El-Naggar, H.A.; El-Damhougy, K.A.; Bashar, M.A.; Ashour, M.; Abo-Taleb, H.A. GC-MS analysis of bioactive components in six different crude extracts from the Soft Coral (*Sinularia maxim*) collected from Ras Mohamed, Aqaba Gulf, Red Sea, Egypt. *Egypt. J. Aquat. Biol. Fish.* **2020**, *24*, 425–434. [[CrossRef](#)]
3. Cui, H.; Bashar, M.A.E.; Rady, I.; Abd El-Naggar, H.; El-Maoula, L.M.A.; Mehany, A.B.M. Antiproliferative Activity, Proapoptotic Effect, and Cell Cycle Arrest in Human Cancer Cells of Some Marine Natural Product Extract. *Oxidative Med. Cell. Longev.* **2020**, *2020*, 7948705. [[CrossRef](#)] [[PubMed](#)]
4. Hasaballah, A.I.; El Naggar, H.A.; Abdelbary, S.; Bashar, M.A.E.; Selim, T.A. Eco friendly Synthesis of Zinc Oxide Nanoparticles by Marine Sponge, *Spongia ofcinalis*: Antimicrobial and Insecticidal Activities against the Mosquito Vectors, *Culex pipiens* and *Anopheles pharoensis*. *BioNanoScience* **2021**. [[CrossRef](#)]
5. Mona, M.H.; El-Naggar, H.; El-Gayar, E.E.; Masood, M.F.; Mohamed, E.-S.N. Effect of human activities on biodiversity in Nabq Protected Area, South Sinai, Egypt. *Egypt. J. Aquat. Res.* **2019**, *45*, 33–43. [[CrossRef](#)]
6. Shaban, W.; Abdel-Gaid, S.E.; El-Naggar, H.A.; Bashar, M.A.; Masood, M.F.; Salem, E.-S.S.; Alabssawy, A.N. Effects of recreational diving and snorkeling on the distribution and abundance of surgeonfishes in the Egyptian Red Sea northern islands. *Egypt. J. Aquat. Res.* **2020**, *46*, 251–257. [[CrossRef](#)]
7. Darweesh, K.F.; Hellal, A.M.; Saber, S.A.; EL-Naggar, H.A.; EL-Kafrawy, S.B. Impact of tourism and fishing on the coral reef health along the west coast of the Gulf of Aqaba, Red Sea, Egypt. *Egypt. J. Aquat. Biol. Fish.* **2021**, *25*, 785–805. [[CrossRef](#)]
8. Dibattista, J.D.; Roberts, M.B.; Bouwmeester, J.; Bowen, B.W.; Coker, D.J.; Lozano-Cortés, D.F.; Choat, J.H.; Gaither, M.R.; Hobbs, J.-P.; Khalil, M.; et al. A review of contemporary patterns of endemism for shallow water reef fauna in the Red Sea. *J. Biogeogr.* **2016**, *43*, 423–439. [[CrossRef](#)]
9. Rady, I.; Siddiqui, I.A.; Rady, M.; Mukhtar, H. Melittin, a major peptide component of bee venom, and its conjugates in cancer therapy. *Cancer Lett.* **2017**, *402*, 16–31. [[CrossRef](#)]
10. Rady, I.; Bloch, M.B.; Chamcheu, R.-C.N.; Mbeumi, S.B.; Anwar, R.; Mohamed, H.; Babatunde, A.S.; Kuate, J.-R.; Noubissi, F.K.; El Sayed, K.A.; et al. Anticancer Properties of Graviola (*Annona muricata*): A Comprehensive Mechanistic Review. *Oxidative Med. Cell. Longev.* **2018**, *2018*, 1826170. [[CrossRef](#)]
11. Orienti, I.; Gentilomi, G.A.; Farruggia, G. Pulmonary Delivery of Fenretinide: A Possible Adjuvant Treatment in COVID-19. *Int. J. Mol. Sci.* **2020**, *21*, 3812. [[CrossRef](#)]
12. Poochi, S.P.; Easwaran, M.; Balasubramanian, B.; Anbuselvam, M.; Meyyazhagan, A.; Park, S.; Bhotla, H.K.; Anbuselvam, J.; Arumugam, V.A.; Keshavarao, S.; et al. Employing bioactive compounds derived from *Ipomoea obscura* (L.) to evaluate potential inhibitor for SARS-CoV-2 main protease and ACE2 protein. *Food Front.* **2020**, *1*, 168–179. [[CrossRef](#)]
13. Gad, A.; Suleiman, W.B.; Beltagy, E.A.; El-Sheikh, H.H.; Ibrahim, H.A.H. Characterization and screening of marine-derived fungi along the coastline of Alexandria, Mediterranean Sea, Egypt. *Egypt. J. Aquat. Biol. Fish.* **2021**, *25*, 215–239. [[CrossRef](#)]
14. Farrag, M.M.S.; El-Naggar, H.; Abou-Mahmoud, M.M.A.; Alabssawy, A.N.; Ahmed, H.O.; Abo-Taleb, H.A.; Kostas, K.; Abo-Taleb, H. Marine biodiversity patterns off Alexandria area, southeastern Mediterranean Sea, Egypt. *Environ. Monit. Assess.* **2019**, *191*, 367. [[CrossRef](#)]
15. Hashem, A.H.; Suleiman, W.B.; Abu-Elrish, G.M.; El-Sheikh, H.H. Consolidated Bioprocessing of Sugarcane Bagasse to Microbial Oil by Newly Isolated Oleaginous Fungus: *Mortierella wolfii*. *Arab. J. Sci. Eng.* **2021**, *46*, 199–211. [[CrossRef](#)]
16. El-Mehdawy, A.A.; Koriem, M.; Amin, R.M.; El-Naggar, H.A.; Shehata, A.Z.I. The photosensitizing activity of different photosensitizers irradiated with sunlight against aquatic larvae of *Culex pipiens* L. (Diptera: Culicidae). *Egypt. J. Aquat. Biol. Fish.* **2021**, *25*, 661–670. [[CrossRef](#)]
17. Hasaballah, A.I.; Gobaara, I.M.M.; El Naggar, H.A. Larvicidal activity and ultrastructural abnormalities in the ovaries of the housefly “*Musca domestica*” induced by the soft coral “*Ovabunda macrospiculata*” synthesized ZnO nanoparticles. *Egypt. J. Aquat. Biol. Fish.* **2021**, *25*, 721–738. [[CrossRef](#)]
18. Moitinho-Silva, L.; Bayer, K.; Cannistraci, C.V.; Giles, E.C.; Ryu, T.; Seridi, L.; Ravasi, T.; Hentschel, U. Specificity and transcriptional activity of microbiota associated with low and high microbial abundance sponges from the Red Sea. *Mol. Ecol.* **2014**, *23*, 1348–1363. [[CrossRef](#)]
19. El-Damhougy, K.A.; El-Naggar, H.A.; Ibrahim, H.A.H.; Bashar, M.A.E.; Abou-Senna, F.M. Biological activities of some marine sponge extracts from Aqaba Gulf, Red Sea, Egypt. *Int. J. Fish. Aquat. Stud.* **2017**, *5*, 652–659.

20. El-Naggar, H.A.; Hasaballah, A.I. Acute larvicidal toxicity and repellency effect of *Octopus cyanea* crude extracts against the filariasis vector, *Culex pipiens*. *J. Egypt. Soc. Parasitol.* **2018**, *48*, 721–728. [CrossRef]
21. Ibrahim, H.A.H.; El-Naggar, H.A.; El-Damhougy, K.A.; Bashar, M.A.E.; Abou-Senna, F.M. *Callyspongia crassa* and *C. siphonella* (Porifera, Callyspongiidae) as a potential source for medical bioactive substances, Aqaba Gulf, Red Sea, Egypt. *J. Basic Appl. Zool.* **2017**, *78*, 7. [CrossRef]
22. El-Damhougy, K.A.; Bashar, M.A.E.; El-Naggar, H.A.; Ibrahim, H.A.H.; Abou Senna, F.M. GC-MS analysis of bioactive components of *Callyspongia crassa* (Porifera) from Gulf of Aqaba, Red Sea (Egypt). *Al-Azhar Bull. Sci.* **2017**, *9*, 111–118.
23. Hasaballah, A.I.; El-Naggar, H.A. Antimicrobial Activities of Some Marine Sponges, and Its Biological, Repellent Effects against *Culex pipiens* (Diptera: Culicidae). *Annu. Res. Rev. Biol.* **2017**, *12*, 1–14. [CrossRef]
24. Lefranc, F.; Nuzzo, G.; Hamdy, N.A.; Fakhr, I.; Banuls, L.M.Y.; Van Goietsenoven, G.; Villani, G.; Mathieu, V.; van Soest, R.; Kiss, R.; et al. In Vitro Pharmacological and Toxicological Effects of Norterpene Peroxides Isolated from the Red Sea Sponge *Diacarnus erythraeanus* on Normal and Cancer Cells. *J. Nat. Prod.* **2013**, *76*, 1541–1547. [CrossRef]
25. Youssef, D.T.A.; Mooberry, S.L. Hurghadolide A and Swinholide I, Potent Actin-Microfilament Disrupters from the Red Sea Sponge *Theonella swinhoei*. *J. Nat. Prod.* **2006**, *69*, 154–157. [CrossRef]
26. Youssef, D.T.A.; Shaala, L.A.; Mohamed, G.A.; Badr, J.M.; Bamanie, F.H.; Ibrahim, S.R.M. Theonellamide G, a Potent Antifungal and Cytotoxic Bicyclic Glycopeptide from the Red Sea Marine Sponge *Theonella swinhoei*. *Mar. Drugs* **2014**, *12*, 1911–1923. [CrossRef]
27. Isaacs, S.; Hizi, A.; Kashman, Y. Toxicols A–C and toxiusol—New bioactive hexaprenoid hydroquinones from *Toxiclona toxius*. *Tetrahedron* **1993**, *49*, 4275–4282. [CrossRef]
28. Shaala, L.A.; Youssef, D.T.A.; Badr, J.M.; Sulaiman, M.; Khedr, A. Bioactive Secondary Metabolites from the Red Sea Marine Verongid Sponge *Suberea* Species. *Mar. Drugs* **2015**, *13*, 1621–1631. [CrossRef]
29. Shaala, L.A.; Youssef, D.T.A. Cytotoxic Psammaphysin Analogues from the Verongid Red Sea Sponge *Aplysinella* Species. *Biomolecules* **2019**, *9*, 841. [CrossRef] [PubMed]
30. Youssef, D.T.A. Hyrtioerectines A–C, Cytotoxic Alkaloids from the Red Sea Sponge *Hyrtios erectus*. *J. Nat. Prod.* **2005**, *68*, 1416–1419. [CrossRef]
31. Youssef, D.T.A.; Yamaki, R.K.; Kelly, M.; Scheuer, P.J. Salmahyrtisol A, a Novel Cytotoxic Sesterterpene from the Red Sea Sponge *Hyrtios erecta*. *J. Nat. Prod.* **2002**, *65*, 2–6. [CrossRef] [PubMed]
32. Alahdal, A.M.; Asfour, H.Z.; Ahmed, S.A.; Noor, A.O.; Al-Abd, A.M.; Elfaky, M.A.; Elhady, S.S. Anti-Helicobacter, Antitubercular and Cytotoxic Activities of Scalaranes from the Red Sea Sponge *Hyrtios erectus*. *Molecules* **2018**, *23*, 978. [CrossRef] [PubMed]
33. Yosief, T.; Rudi, A.; Kashman, Y. Asmarines A–F, Novel Cytotoxic Compounds from the Marine Sponge *Raspailia* Species. *J. Nat. Prod.* **2000**, *63*, 299–304. [CrossRef] [PubMed]
34. Grkovic, T.; Abdelmohsen, U.R.; Othman, E.M.; Stopper, H.; Edrada-Ebel, R.; Hentschel, U.; Quinn, R.J. Two new antioxidant actinosporin analogues from the calcium alginate beads culture of sponge-associated *Actinokineospora* sp. strain EG49. *Bioorg. Med. Chem. Lett.* **2014**, *24*, 5089–5092. [CrossRef]
35. Jomori, T.; Shiroyama, S.; Ise, Y.; Kohtsuka, H.; Matsuda, K.; Kuranaga, T.; Wakimoto, T. Scrobiculosides A and B from the deep-sea sponge *Pachastrella scrobiculosa*. *J. Nat. Med.* **2019**, *73*, 814–819. [CrossRef]
36. Li, F.; Peifer, C.; Janussen, D.; Tasdemir, D. New Discorhabdin Alkaloids from the Antarctic Deep-Sea Sponge *Latrunculia biformis*. *Mar. Drugs* **2019**, *17*, 439. [CrossRef]
37. Rubin-Blum, M.; Antony, C.P.; Sayavedra, L.; Martínez-Pérez, C.; Birgel, D.; Peckmann, J.; Wu, Y.-C.; Cardenas, P.; Macdonald, I.; Marcon, Y.; et al. Fueled by methane: Deep-sea sponges from asphalt seeps gain their nutrition from methane-oxidizing symbionts. *ISME J.* **2019**, *13*, 1209–1225. [CrossRef]
38. Ayyad, S.-E.N.; Angawi, R.F.; Saqer, E.; Abdel-Lateff, A.; Badria, F.A. Cytotoxic neviotane triterpene-type from the red sea sponge *Siphonochalina siphonella*. *Pharmacogn. Mag.* **2014**, *10*, 334–341. [CrossRef]
39. El-Hawary, S.S.; Sayed, A.M.; Mohammed, R.; Hassan, H.M.; Rateb, M.E.; Amin, E.; Mohammed, T.A.; El-Mesery, M.; Bin Muhsinah, A.; Alsayari, A.; et al. Bioactive Brominated Oxindole Alkaloids from the Red Sea Sponge *Callyspongia siphonella*. *Mar. Drugs* **2019**, *17*, 465. [CrossRef]
40. Youssef, D.T.A.; van Soest, R.W.M.; Fusetani, N. Callyspongenols A–C, New Cytotoxic C22-Polyacetylenic Alcohols from a Red Sea Sponge, *Callyspongia* Species. *J. Nat. Prod.* **2003**, *66*, 679–681. [CrossRef]
41. Youssef, D.T.A.; van Soest, R.W.M.; Fusetani, N. Callyspongamide A, a New Cytotoxic Polyacetylenic Amide from the Red Sea Sponge *Callyspongia fistularis*. *J. Nat. Prod.* **2003**, *66*, 861–862. [CrossRef]
42. Abdelmohsen, U.R.; Cheng, C.; Reimer, A.; Kozjak-Pavlovic, V.; Ibrahim, A.K.; Rudel, T.; Hentschel, U.; Edrada-Ebel, R.; Ahmed, S.A. Antichlamydial Sterol from the Red Sea Sponge *Callyspongia* aff. *implexa*. *Planta Med.* **2015**, *81*, 382–387. [CrossRef]
43. Hooper, J.N.A. *Spongicide: Guide to Sponge Collection and Identification Version*; Queensland Museum: South Brisbane, QLD, Australia, 2000; p. 210.
44. Van Soest, R.W.M.; Boury-Esnault, N.; Hooper, J.N.A.; Rützler, K.; de Voogd, N.J.; Alvarez, B.; Hajdu, E.; Pisera, A.B.; Manconi, R.; Schönberg, C.; et al. World Porifera Database. 2021. Available online: <http://www.marinespecies.org/porifera/> (accessed on 19 January 2022).

45. Attia, M.S.; El-Naggar, H.A.; Abdel-Daim, M.M.; El-Sayyad, G.S. The potential impact of Octopus cyanea extracts to improve eggplant resistance against Fusarium-wilt disease: In vivo and in vitro studies. *Environ. Sci. Pollut. Res.* **2021**, *28*, 35854–35869. [[CrossRef](#)]
46. Chamcheu, J.C.; Rady, I.; Chamcheu, R.-C.N.; Siddique, A.B.; Bloch, M.B.; Banang Mbeumi, S.; Babatunde, A.S.; Uddin, M.B.; Noubissi, F.K.; Jurutka, P.W.; et al. Graviola (*Annona muricata*) Exerts Anti-Proliferative, Anti-Clonogenic and Pro-Apoptotic Effects in Human Non-Melanoma Skin Cancer UW-BCC1 and A431 Cells In Vitro: Involvement of Hedgehog Signaling. *Int. J. Mol. Sci.* **2018**, *19*, 1791. [[CrossRef](#)]
47. Suleiman, W.B.; Helal, E.E.-H. Chemical constituents and potential pleiotropic activities of *Foeniculum vulgare* (Fennel) ethanolic extract; in vitro approach. *Egypt. J. Chem.* **2022**, *65*, 5. [[CrossRef](#)]
48. Luparello, C.; Ragona, D.; Asaro, D.M.L.; Lazzara, V.; Affranchi, F.; Celi, M.; Arizza, V.; Vazzana, M. Cytotoxic Potential of the Coelomic Fluid Extracted from the Sea Cucumber *Holothuria tubulosa* against Triple-Negative MDA-MB231 Breast Cancer Cells. *Biology* **2019**, *8*, 76. [[CrossRef](#)]
49. Sanna, V.; Singh, C.K.; Jashari, R.; Adhami, V.M.; Chamcheu, J.C.; Rady, I.; Sechi, M.; Mukhtar, H.; Siddiqui, I.A. Targeted nanoparticles encapsulating (–)-epigallocatechin-3-gallate for prostate cancer prevention and therapy. *Sci. Rep.* **2017**, *7*, 41573. [[CrossRef](#)]
50. Xu, W.; Siddiqui, I.A.; Nihal, M.; Pilla, S.; Rosenthal, K.; Mukhtar, H.; Gong, S. Aptamer-conjugated and doxorubicin-loaded unimolecular micelles for targeted therapy of prostate cancer. *Biomaterials* **2013**, *34*, 5244–5253. [[CrossRef](#)]
51. Kim, K.H.; Sederstrom, J.M. Assaying Cell Cycle Status Using Flow Cytometry. *Curr. Protoc. Mol. Biol.* **2015**, *111*, 28.6.1–28.6.11. [[CrossRef](#)]
52. Crowley, L.; Marfell, B.J.; Scott, A.P.; Waterhouse, N.J. Quantitation of Apoptosis and Necrosis by Annexin V Binding, Propidium Iodide Uptake, and Flow Cytometry. *Cold Spring Harb. Protoc.* **2016**, 2016. [[CrossRef](#)]
53. Degl'Innocenti, D.; Ramazzotti, M.; Sarchielli, E.; Monti, D.; Chevanne, M.; Vannelli, G.B.; Barletta, E. Oxadiazon affects the expression and activity of aldehyde dehydrogenase and acylphosphatase in human striatal precursor cells: A possible role in neurotoxicity. *Toxicology* **2019**, *411*, 110–121. [[CrossRef](#)]
54. Kamel, A.; Suleiman, W.B.; Elfeky, A.; El-Sherbiny, G.M.; Elhaw, M. Characterization of bee venom and its synergistic effect combating antibiotic resistance of *Pseudomonas aeruginosa*. *Egypt. J. Chem.* **2021**, *65*. [[CrossRef](#)]
55. Suleiman, W.B. In vitro estimation of superfluid critical extracts of some plants for their antimicrobial potential, phytochemistry, and GC-MS analyses. *Ann. Clin. Microbiol. Antimicrob.* **2020**, *19*, 29. [[CrossRef](#)]
56. Yang, R.; Johnson, M.C.; Ray, B. Novel method to extract large amounts of bacteriocins from lactic acid bacteria. *Appl. Environ. Microbiol.* **1992**, *58*, 3355–3359. [[CrossRef](#)]
57. Li, H.; Gao, T.; Wang, J.; Tian, S.; Yuan, X.; Zhu, H. Structural identification and antitumor activity of the extracellular polysaccharide from *Aspergillus terreus*. *Process. Biochem.* **2016**, *51*, 1714–1720. [[CrossRef](#)]
58. Domenici, L.; Monti, M.; Bracchi, C.; Giorgini, M.; Colagiovanni, V.; Muzii, L.; Panici, P.B. D-mannose: A promising support for acute urinary tract infections in women. A pilot study. *Eur. Rev. Med. Pharmacol. Sci.* **2016**, *20*, 2920–2925.
59. Wang, B.; Peng, X.-X.; Sun, R.; Li, J.; Zhan, X.-R.; Wu, L.-J.; Wang, S.-L.; Xie, T. Systematic review of  $\beta$ -Elemene injection as adjunctive treatment for lung cancer. *Chin. J. Integr. Med.* **2012**, *18*, 813–823. [[CrossRef](#)]
60. Santana de Oliveira, M.; da Cruz, J.N.; Almeida da Costa, W.; Silva, S.G.; Brito, M.d.P.; de Menezes, S.A.F.; de Jesus Chaves Neto, A.M.; de Aguiar Andrade, E.H.; de Carvalho Junior, R.N. Chemical Composition, Antimicrobial Properties of *Siparuna guianensis* Essential Oil and a Molecular Docking and Dynamics Molecular Study of its Major Chemical Constituent. *Molecules* **2020**, *25*, 3852. [[CrossRef](#)]
61. Do Nascimento, K.F.; Moreira, F.M.F.; Santos, J.A.; Kassuya, C.A.L.; Croda, J.H.R.; Cardoso, C.A.L.; Vieira, M.D.C.; Ruiz, A.L.T.G.; Foglio, M.A.; de Carvalho, J.E.; et al. Antioxidant, anti-inflammatory, antiproliferative and antimycobacterial activities of the essential oil of *Psidium guineense* Sw. and spathulenol. *J. Ethnopharmacol.* **2018**, *210*, 351–358. [[CrossRef](#)]
62. Manoj, G.; Manohar, S.H.; Murthy, H.N. Chemical constituents, antioxidant and antimicrobial activity of essential oil of *Pogostemon paniculatus* (Willd.). *Nat. Prod. Res.* **2012**, *26*, 2152–2154. [[CrossRef](#)]
63. Elshamy, A.I.; El Kashak, W.; Abdallah, H.; Farrag, A.H.; Nassar, M.I. Soft coral *Cespitularia stolonifera*: New cytotoxic ceramides and gastroprotective activity. *Chin. J. Nat. Med.* **2017**, *15*, 105–114. [[CrossRef](#)]
64. Yasa, S.R.; Kaki, S.S.; Poornachandra, Y.; Kumar, C.G.; Penumarthy, V. Synthesis, characterization, antimicrobial and biofilm inhibitory studies of new esterquats. *Bioorg. Med. Chem. Lett.* **2016**, *26*, 1978–1982. [[CrossRef](#)] [[PubMed](#)]
65. Krishnaveni, M. Docking, simulation studies of desulphosinigrin—Cyclin dependent kinase 2, an anticancer drug target. *Int. J. Pharm. Sci. Rev. Res.* **2015**, *30*, 115–118.
66. Kumar, P.; Sati, S.C.; Khulbe, K.; Pant, P.; Tripathi, A.N.; Sarvendra, K. Phytochemical constituents, antimicrobial and antioxidant activities of Kumaun Himalayan Hoop Pine bark extract. *Nat. Prod. Res.* **2020**, *29*, 1–5. [[CrossRef](#)]
67. Li, K.; Ma, T.; Cai, J.; Huang, M.; Guo, H.; Zhou, D.; Luan, S.; Yang, J.; Liu, D.; Jing, Y.; et al. Conjugates of 18 $\beta$ -glycyrrhetic acid derivatives with 3-(1H-benzo[d]imidazol-2-yl)propanoic acid as Pin1 inhibitors displaying anti-prostate cancer ability. *Bioorg. Med. Chem.* **2017**, *25*, 5441–5451. [[CrossRef](#)]
68. Salomón, D.G.; Grioli, S.M.; Buschiazzo, M.; Mascaró, E.; Vitale, C.; Radivoy, G.; Pérez, M.; Fall, Y.; Mesri, E.A.; Curino, A.C.; et al. Novel Alkynylphosphonate Analogue of Calcitriol with Potent Antiproliferative Effects in Cancer Cells and Lack of Calcemic Activity. *ACS Med. Chem. Lett.* **2011**, *2*, 503–508. [[CrossRef](#)]

69. Santini, V.; Scappini, B.; Gozzini, A.; Grossi, A.; Villa, P.; Ronco, G.; Douillet, O.; Pouillart, P.; Bernabei, P.A.; Ferrini, P.R. Butyrate-stable monosaccharide derivatives induce maturation and apoptosis in human acute myeloid leukaemia cells. *Br. J. Haematol.* **1998**, *101*, 529–538. [[CrossRef](#)]
70. Karrys, A.; Rady, I.; Chamcheu, R.-C.N.; Sabir, M.S.; Mallick, S.; Chamcheu, J.C.; Jurutka, P.W.; Haussler, M.R.; Whitfield, G.K. Bioactive Dietary VDR Ligands Regulate Genes Encoding Biomarkers of Skin Repair That Are Associated with Risk for Psoriasis. *Nutrients* **2018**, *10*, 174. [[CrossRef](#)]
71. Su, C.-T.; Hsu, J.T.-A.; Hsieh, H.-P.; Lin, P.-H.; Chen, T.-C.; Kao, C.-L.; Lee, C.-N.; Chang, S.-Y. Anti-HSV activity of digitoxin and its possible mechanisms. *Antivir. Res.* **2008**, *79*, 62–70. [[CrossRef](#)]
72. Trenti, A.; Boscaro, C.; Tedesco, S.; Cignarella, A.; Trevisi, L.; Bolego, C. Effects of digitoxin on cell migration in ovarian cancer inflammatory microenvironment. *Biochem. Pharmacol.* **2018**, *154*, 414–423. [[CrossRef](#)]
73. López-Lara, I.; Nogales, J.; Pech-Canul, A.D.L.C.; Calatrava-Morales, N.; Bernabéu-Roda, L.M.; Durán, P.; Cuéllar, V.; Olivares, J.; Alvarez, L.; Palenzuela-Bretones, D.; et al. 2-Tridecanone impacts surface-associated bacterial behaviours and hinders plant–bacteria interactions. *Environ. Microbiol.* **2018**, *20*, 2049–2065. [[CrossRef](#)]
74. Swantara, M.D.; Rita, W.S.; Suartha, N.; Agustina, K.K. Anticancer activities of toxic isolate of *Xestospongia testudinaria* sponge. *Vet. World* **2019**, *12*, 1434–1440. [[CrossRef](#)]
75. Abou-El-Wafa, G.S.E.; Shaaban, M.; Shaaban, K.A.; El-Naggar, M.E.E.; Maier, A.; Fiebig, H.H.; Laatsch, H. Pachydictyols B and C: New Diterpenes from *Dictyota dichotoma* Hudson. *Mar. Drugs* **2013**, *11*, 3109–3123. [[CrossRef](#)]
76. Figueiredo, C.R.; Matsuo, A.L.; Massaoka, M.H.; Girola, N.; Azevedo, R.A.; Rabaça, A.N.; Farias, C.F.; Pereira, F.V.; Matias, N.S.; Silva, L.P.; et al. Antitumor Activity of *Kielmeyera coriacea* Leaf Constituents in Experimental Melanoma, Tested in Vitro and in Vivo in Syngeneic Mice. *Adv. Pharm. Bull.* **2014**, *4* (Suppl. 1), 429–436. [[CrossRef](#)]
77. Gelmann, E.P.; Cronan, J.E., Jr. Mutant of *Escherichia coli* deficient in the synthesis of *cis*-vaccenic acid. *J. Bacteriol.* **1972**, *112*, 381–387. [[CrossRef](#)]
78. Kasanah, N.; Amelia, W.; Mukminin, A.; Triyanto; Isnansetyo, A. Antibacterial activity of Indonesian red algae *Gracilaria edulis* against bacterial fish pathogens and characterization of active fractions. *Nat. Prod. Res.* **2019**, *33*, 3303–3307. [[CrossRef](#)]
79. Khosravani, M.; Dallal, M.M.S.; Norouzi, M. Phytochemical Composition and Anti-efflux Pump Activity of Hydroalcoholic, Aqueous, and Hexane Extracts of *Artemisia tournefortiana* in Ciprofloxacin-Resistant Strains of *Salmonella enterica* Serotype Enteritidis. *Iran. J. Public Health* **2020**, *49*, 134–144. [[CrossRef](#)]
80. Joel, J.T.; Suluvoy, J.K.; Raja, R.H. *Morinda citrifolia* L. (Noni) as a free radical scavenger and an anticancer agent. *Drug Invent. Today* **2018**, *10*, 3134–3140.
81. Zhang, Y.; Miller, R.M. Enhanced octadecane dispersion and biodegradation by a *Pseudomonas rhamnolipid* surfactant (biosurfactant). *Appl. Environ. Microbiol.* **1992**, *58*, 3276–3282. [[CrossRef](#)]
82. Mody, N.; Mcilroy, G.D. The mechanisms of Fenretinide-mediated anti-cancer activity and prevention of obesity and type-2 diabetes. *Biochem. Pharmacol.* **2014**, *91*, 277–286. [[CrossRef](#)]
83. Goossens, J.-F.; Bailly, C. Ursodeoxycholic acid and cancer: From chemoprevention to chemotherapy. *Pharmacol. Ther.* **2019**, *203*, 107396. [[CrossRef](#)]
84. Choi, J.-M.; Lee, E.-O.; Lee, H.-J.; Kim, K.-H.; Ahn, K.-S.; Shim, B.-S.; Kim, N.-I.; Song, M.-C.; Baek, N.-I.; Kim, S.-H. Identification of campesterol from *Chrysanthemum coronarium* L. and its antiangiogenic activities. *Phytother. Res.* **2007**, *21*, 954–959. [[CrossRef](#)]
85. Mekhtiev, A.R.; Timofeev, V.P.; Misharin, A.I. (22R,23R)-3beta-Hydroxy-22,23-epoxy-5alpha-ergost-8(14)-en-15-one: Improved synthesis and toxicity to MCF-7 cells. *Bioorg. Khim.* **2008**, *34*, 840–846.
86. Shawli, G.T.; Adeyemi, O.O.; Stonehouse, N.J.; Herod, M.R. The Oxysterol 25-Hydroxycholesterol Inhibits Replication of Murine Norovirus. *Viruses* **2019**, *11*, 97. [[CrossRef](#)]
87. Wang, C.; He, H.; Fang, W. Oncogenic roles of the cholesterol metabolite 25-hydroxycholesterol in bladder cancer. *Oncol. Lett.* **2020**, *19*, 3671–3676. [[CrossRef](#)]
88. Pandey, P.; Bajpai, P.; Siddiqui, M.H.; Sayyed, U.; Tiwari, R.; Shekh, R.; Mishra, K.; Kapoor, V. Elucidation of the Chemopreventive Role of Stigmasterol against Jab1 in Gall Bladder Carcinoma. *Endocr. Metab. Immune Disord. Drug Targets* **2019**, *19*, 826–837. [[CrossRef](#)]
89. Yenn, T.W.; Khan, M.A.; Syuhada, N.A.; Ring, L.C.; Ibrahim, D.; Tan, W.-N. Stigmasterol: An adjuvant for beta lactam antibiotics against beta-lactamase positive clinical isolates. *Steroids* **2017**, *128*, 68–71. [[CrossRef](#)]
90. Bin Sayeed, M.S.; Ameen, S.S. Beta-Sitosterol: A Promising but Orphan Nutraceutical to Fight against Cancer. *Nutr. Cancer* **2015**, *67*, 1216–1222. [[CrossRef](#)] [[PubMed](#)]
91. Sundarraj, S.; Thangam, R.; Sreevani, V.; Kaveri, K.; Gunasekaran, P.; Achiraman, S.; Kannan, S.  $\gamma$ -Sitosterol from *Acacia nilotica* L. induces G2/M cell cycle arrest and apoptosis through c-Myc suppression in MCF-7 and A549 cells. *J. Ethnopharmacol.* **2012**, *141*, 803–809. [[CrossRef](#)] [[PubMed](#)]
92. Thakur, R.S.; Ahirwar, B. A steroidal derivative from *Trigonella foenum graecum* L. that induces apoptosis in vitro and in vivo. *J. Food Drug Anal.* **2019**, *27*, 231–239. [[CrossRef](#)] [[PubMed](#)]
93. Gallup, J.M.; Grubor, B.; Barua, A.B.; Mohammadi, G.; Brogden, K.A.; Olson, J.A.; Ackermann, M.R. Repeated intravenous doses of all-trans-retinoyl beta-D-glucuronide is not effective in the treatment of bacterial bronchopneumonia in lambs but is devoid of gross and acute toxicity. *Med. Sci. Monit.* **2002**, *8*, 345–353.

94. Jainab, N.H.; Raja, M. In vitro cytotoxic, antioxidant and GC-MS study of leaf extracts of *Clerodendrum phlomidis*. *Int. J. Pharm. Sci. Res.* **2017**, *8*, 4433–4440. [[CrossRef](#)]
95. Suleiman, W.B.; El Bous, M.M.; El Said, M.; El Baz, H. In vitro evaluation of *Syzygium aromaticum* L. ethanol extract as biocontrol agent against postharvest tomato and potato diseases. *Egypt. J. Bot.* **2019**, *59*, 81–94. [[CrossRef](#)]
96. Abubacker, M.N.; Devi, P.K. In vitro antifungal potentials of bioactive compound oleic acid, 3-(octadecyloxy) propyl ester isolated from *Lepidagathis cristata* Willd. (Acanthaceae) inflorescence. *Asian Pac. J. Trop. Med.* **2014**, *7* (Suppl. 1), S190–S193. [[CrossRef](#)]
97. Kim, N.Y.; Choi, W.Y.; Heo, S.J.; Kang, D.H.; Lee, H.Y. Anti-Skin Cancer Activities of *Apostichopus japonicus* Extracts from Low-Temperature Ultrasonification Process. *J. Health Eng.* **2017**, *2017*, 6504890. [[CrossRef](#)]
98. Du, L.; Li, Z.-J.; Xu, J.; Wang, J.-F.; Xue, Y.; Xue, C.-H.; Takahashi, K.; Wang, Y.-M. The anti-tumor activities of cerebrosides derived from sea cucumber *Acaudina molpadioides* and starfish *Asterias amurensis* in vitro and in vivo. *J. Oleo Sci.* **2012**, *61*, 321–330. [[CrossRef](#)]
99. Zakaria, H.Y.; El-Naggar, H. Long-term variations of zooplankton community in Lake Edku, Egypt. *Egypt. J. Aquat. Biol. Fish.* **2019**, *23*, 215–226. [[CrossRef](#)]
100. Chari, A.; Mazumder, A.; Lau, K.; Catamero, D.; Galitzcek, Z.; Jagannath, S. A phase II trial of TBL-12 sea cucumber extract in patients with untreated asymptomatic myeloma. *Br. J. Haematol.* **2018**, *180*, 296–298. [[CrossRef](#)]
101. Dhinakaran, D.I.; Lipton, A.P. Antimicrobial potential of the marine sponge *Sigmadocia pumila* from the south eastern region of India. *World J. Fish Mar. Sci.* **2012**, *4*, 344–348. [[CrossRef](#)]
102. Gab-Alla, A.A.F.A.; Kilada, R.W.; Shalaby, I.M.; Helmy, T. Antimicrobial activity of some sponges from the Gulf of Aqaba. *Egypt. J. Biol.* **2000**, *2*, 28–33. Available online: <https://www.ajol.info/index.php/ejb/article/view/29901> (accessed on 22 January 2022).
103. Shawky, M.; Suleiman, W.B.; Farrag, A.A. Antibacterial Resistance Pattern in Clinical and Non-clinical Bacteria by Phenotypic and Genotypic Assessment. *J. Pure Appl. Microbiol.* **2021**, *15*, 2270–2279. [[CrossRef](#)]
104. Soliman, M.O.; Suleiman, W.B.; Roushdy, M.M.; Elbatrawy, E.N.; Gad, A.M. Characterization of some bacterial strains isolated from the Egyptian Eastern and Northern coastlines with antimicrobial activity of *Bacillus zhangzhouensis* OMER4. *Acta Oceanol. Sin.* **2021**, *41*, 1–8. [[CrossRef](#)]
105. Gad, A.M.; Suleiman, W.B.; Beltagy, E.A.; El-Sheikh, H.; Ibrahim, H.A. Antimicrobial and antifouling activities of the cellulase produced by marine fungal strain; *Geotrichum candidum* MN638741.1. *Egypt. J. Aquat. Biol. Fish.* **2021**, *25*, 49–60. [[CrossRef](#)]
106. Saleem, M.D.; Feldman, S.R. Desoximetasone 0.25% spray, adrenal suppression and efficacy in extensive plaque psoriasis. *J. Dermatol. Treat.* **2018**, *29*, 36–38. [[CrossRef](#)] [[PubMed](#)]
107. Saleem, M.D.; Negus, D.; Feldman, S.R. Topical 0.25% desoximetasone spray efficacy for moderate to severe plaque psoriasis: A randomized clinical trial. *J. Dermatol. Treat.* **2018**, *29*, 32–35. [[CrossRef](#)] [[PubMed](#)]
108. Al-Rabia, M.W.; Mohamed, G.A.; Ibrahim, S.R.M.; Asfour, H.Z. Anti-inflammatory ergosterol derivatives from the endophytic fungus *Fusarium chlamydosporum*. *Nat. Prod. Res.* **2020**, *35*, 5011–5020. [[CrossRef](#)]
109. El-Naggar, H.; Allah, H.M.K.; Masood, M.F.; Shaban, W.M.; Bashar, M.A. Food and feeding habits of some Nile River fish and their relationship to the availability of natural food resources. *Egypt. J. Aquat. Res.* **2019**, *45*, 273–280. [[CrossRef](#)]
110. Zakaria, H.Y.; Hassan, A.-K.M.; Abo-Senna, F.M.; El-Naggar, H. Abundance, distribution, diversity and zoogeography of epipelagic copepods off the Egyptian Coast (Mediterranean Sea). *Egypt. J. Aquat. Res.* **2016**, *42*, 459–473. [[CrossRef](#)]
111. Zakaria, H.Y.; Hassan, A.-K.M.; El-Naggar, H.A.; Abo-Senna, F.M. Biomass determination based on the individual volume of the dominant copepod species in the Western Egyptian Mediterranean Coast. *Egypt. J. Aquat. Res.* **2018**, *44*, 89–99. [[CrossRef](#)]
112. Abdel-Razek, A.; El-Sheikh, H.; Suleiman, W.; Taha, T.H.; Mohamed, M. Bioelimination of phenanthrene using degrading bacteria isolated from petroleum soil: Safe approach. *Desalin. Water Treat.* **2020**, *181*, 131–140. [[CrossRef](#)]